Mineral. Soc. Amer. Spec. Pap. **2,** 117–136 (1969).

CRYSTAL-CHEMICAL CHARACTERIZATION OF CLINOAMPHIBOLES BASED ON FIVE NEW STRUCTURE REFINEMENTS[1]

J. J. Papike, Malcolm Ross, and Joan R. Clark
U. S. Geological Survey, Washington, D.C. 20242

Abstract

Five new structural refinements of tremolite, *C*-centered manganoan cummingtonite, primitive manganoan cummingtonite, hornblende and potassic richterite are compared with published results for cummingtonite, grunerite and glaucophane. The nature of the cation species occupying the $M(4)$ site is of key importance in amphibole phase relations. The differences between the $M(4)$-O coordination polyhedra for (Mg, Fe^{2+}, Mn)-clinoamphiboles and (Ca, Na)-clinoamphiboles are largely responsible for the limited miscibility between these amphibole groups at low temperatures. The presence of Mg in the $M(4)$ site, sometimes also with Ca or Na, is considered responsible for the occurrence of the primitive clinoamphibole structure with space group $P2_1/m$. In this structure there are two crystallographically independent tetrahedral chains, one of which is relatively straight, and the other, kinked. The *A* site is occupied by K in potassic-richterite and by (Na, K) in the Kakanui hornblende. A split-atom model, indicating either positional or thermal disorder around the *A* site central point, best fits the data and indicates eight-fold coordination of K out to 3.00 Å, rather than six-fold as for K in micas. In the aluminous hornblende the $T(1)$ tetrahedron is enriched in Al relative to $T(2)$. In tremolite the hydrogen atom is located on the mirror plane, the O3-H distance is 0.85(7) Å, and the angle to the octahedral strip is 94°. Refinement of anisotropic thermal parameters for each atom of tremolite shows that only the Ca atom has marked anisotropy.

Introduction

Although the basic features of the clinoamphibole crystal structure were illustrated by Warren in 1929, many problems in amphibole crystal chemistry remain today and some of these are considered in this paper. Important contributions to the understanding of amphibole crystal structures have been made by studies of magnesio-riebeckite (Whittaker, 1949), actinolite (Zussman, 1955), hornblendes (Heritsch, *et al.,* 1957, 1960; Heritsch and Kahler, 1960; Heritsch and Riechert, 1960), tremolite (Zussman, 1959), grunerite (Ghose and Hellner, 1959; Finger and Zoltai, 1967), cummingtonite (Ghose, 1961; Fischer, 1966), arfvedsonite (Kawahara, 1963), two synthetic amphiboles (Prewitt, 1963), riebeckite (Colville and Gibbs, 1964) and glaucophane (Papike and Clark, 1968). We now report new crystal-structure refinements for five amphiboles: tremolite, *C*-centered manganoan cummingtonite, primitive manganoan cummingtonite, a hornblende rich in K and Al and potassic richterite. These new refinement results are compared with previous results for cummingtonite (Ghose, 1961), grunerite (Finger and Zoltai, 1967) and glaucophane (Papike and Clark, 1968), which are the only other published refinements carried out by modern techniques.

Crystals for each of the new refinements were chosen so information would be obtained about particular amphibole crystal-chemical problems. Tremolite was selected to examine the details of the calcic clinoamphibole "type structure". *C*-centered manganoan cummingtonite was selected to help explain the distribution of Mn^{2+}, Fe^{2+} and Mg over the four clinoamphibole *M*-sites, and to provide data complementary to spectral studies (Bancroft, Burns and Maddock, 1967) and previous X-ray diffraction studies (already cited) on grunerite-cummingtonite crystalline solutions. The results are also essential to the understanding of primitive manganoan cummingtonite, which was selected for study because it represents a new clinoamphibole structure type (Bown, 1965). This new amphibole is found as an exsolved phase from many calcic amphibole host crystals (Ross, Papike and Weiblen, 1968; Ross, Papike and Shaw, 1969, this volume). A hornblende rich in K and Al was chosen to provide information about Na and K coordination in the amphibole *A* site and the distribution of tetrahedral aluminum between the $T(1)$ and $T(2)$ sites. Potassic richterite was selected because its *A* site is filled with potassium, so the coordination of potassium in the clinoamphibole structure could be examined and compared with that in the feldspar and mica structures. These various problems are considered in turn in the remainder of this report, and the important conclusions resulting from comparison of eight clinoamphibole refinements are summarized at the end.

Experimental Data

Crystallographic data, origin of the crystals used for the structural analyses, and information about the unit-cell contents and the method of calculation are summarized in Table 1. The complete data for chemical analyses are available in the given references (Table 1); new analyses for tremolite and primitive manganoan cummingtonite are reported by Ross, Papike and Shaw (1969, this volume). The reliability of the analysis for the Australian potassic richterite (Prider, 1939) was confirmed by electron-microprobe analysis carried out by A. T. Anderson, U. S. Geological Survey. Collection and processing of the intensity data were handled as described by Clark, Appleman and Papike (1969), and information specific to the amphibole crystals is given in Table 2, where the final *R* values and the standard deviations in $|F|$ are listed. The *R* given is $\Sigma||F_o| - |F_c||/\Sigma|F_o|$.

For the refinement of primitive manganoan cummingtonite, initial atomic parameters were taken from the published refinement of cummingtonite (Ghose, 1961), appropriately modified to allow for the $P2_1/m$ symmetry requirements. The starting parameters for the *C*-centered manganoan cummingtonite refinement were also taken from Ghose (1961). The glaucophane

---

[1] Studies of silicate minerals (14). Publication authorized by the Director, U. S. Geological Survey.

TABLE 1. CRYSTAL DATA FOR EIGHT MONOCLINIC AMPHIBOLES

	Tremolite Present study	Cummingtonite Ghose (1961); Fischer(1966)	Grunerite Finger and Zoltai (1967)	*C*-centered Manganoan cummingtonite Present study	Glaucophane Papike and Clark (1968)	Hornblende Present study	Potassic richterite Present study	Primitive manganoan cummingtonite Present study
a (Å)	9.818(5)	9.51	9.5642(7)	9.583(2)	9.541(2)	9.870(1)	10.019(2)	9.550(1)
b (Å)	18.047(8)	18.19	18.393(2)	18.091(5)	17.740(3)	18.058(4)	18.036(7)	18.007(3)
c (Å)	5.275(3)	5.33	5.3388(3)	5.315(4)	5.295(2)	5.307(2)	5.286(3)	5.298(1)
β	104°39′(3)′	101°55′	101°53.5′(2)	102°38′(1)	103°40′(1)	105°12′(1)	104°59′(2)	102°39′(1)
Cell Volume (Å^3)	904.2(6)	[902.1]	919.0(2)	899.1(6)	870.9(3)	912.7(3)	922.7(3)	888.9(2)
Space Group	$C2/m$	$C2/m$	$C2/m$	$C2/m$	$C2/m$	$C2/m$	$C2/m$	$P2_1/m$
Unit-Cell Contents								
Si	7.95	7.90	8.00	7.95	7.92	5.97	7.44	8.02
Al^{IV}	0.05	0.10	—	0.05	0.08	2.03	0.29	—
Fe^{3+}	—	—	—	—	—	—	0.06	—
Ti	—	—	—	—	—	—	0.21	—
Tetrahedral Σ	8.00	8.00	8.00	8.00	8.00	8.00	8.00	8.02
Al^{VI}	0.04	—	—	—	1.58	0.39	—	0.01
Mg	4.97	4.05	0.77	4.11	2.38	2.85	4.49	5.57
Fe^{2+}	0.02	2.50	6.14	0.54	0.70	0.84	0.28	0.01
Fe^{3+}	—	—	—	—	0.30	0.54	—	—
Mn	0.05	0.17	0.05	2.02	0.01	0.01	0.01	0.96
Ti	—	—	—	—	0.06	0.49	0.17	—
Octahedral Σ	5.08	6.72	6.96	6.67	5.03	5.12	4.95	6.55
Ca	1.86	0.35	0.06	0.18	0.20	1.63	1.05	0.36
Na	0.10	—	—	0.03	1.84	0.87	1.00	0.06
K	0.02	—	—	—	—	0.39	1.03	—
Large Cations Σ	1.98	0.35	0.06	0.21	2.04	2.89	3.08	0.42
Z	2	2	2	2	2	2	2	2
Calc. Density g/cm^3	2.99	3.21	3.54	3.18	3.13	3.23	3.08	3.05
Locality and references	Gouverneur, New York, Mining District	Iron formation, Quebec	Wabush Iron Formation, Labrador, Canada	Wabush Iron Formation, Labrador, Canada	Glaucophane schist, Tiburon Peninsula, California	Volcanic breccia, Kakanui, New Zealand	Potassic volcanics, West Kimberly area, Western Australia	Gouverneur, New York Talc District
	Ross, Smith, Ashton (1968), Sample G-21	Ghose (1961)	Klein (1964), Sample No. 1; Finger and Zoltai (1967)	Klein (1964), Sample No. 2	Papike and Clark (1968)	Mason (1966); Papike and Clark (1967); Mason (1968)	Prider (1939); Papike, Clark, Huebner (1968)	Segeler (1961), USNM 115046; Ross, Papike, Weiblen (1968); Papike, Ross, Clark (1968)
Information on analysis	Ross *et al.* (1969, this volume)	Ghose (1961)	Klein (1964)	Klein (1964)	Papike and Clark (1968)	Mason (1968)	Prider (1939)	Ross *et al.* (1969, this volume)
Calculation based on	23 oxygens	not given	24 (O, OH, F)	24 (O, OH, F)	24 (O, OH, F, Cl)	Total cations normalized to 16	23 oxygens	23 oxygens

parameters (Papike and Clark, 1968) were used initially in the refinements of tremolite and hornblende and the refined hornblende parameters were then used to initiate the potassic richterite refinement. The computer programs used for least-squares refinement, calculation of electron-density maps, and bond distances and angles were from J. M. Stewart's (Univ. Maryland) *X-Ray 67, Program System for X-Ray Crystallography* (1967), adapted by D. E. Appleman, U.S. Geological Survey, for the IBM 360/65. Atomic scattering factors were taken from MacGillavry and Rieck (1962).

Throughout the refinements, unit weights were used, for reasons discussed by Clark, Appleman and Papike (1969). No corrections were made for either primary or secondary extinction effects, but no reflections appeared to be affected by the former. A very few strong intensities swamped the scintillation counter, and these values were removed from the final cycles of refinement. Positional parameters and individual anisotropic temperature factors were refined for all five structures, but the anisotropic thermal data are presented here only for tremolite which is fully ordered. The temperature factor form used was

$$\exp\left\{-\sum_{i=1}^{3}\sum_{j=1}^{3} \mathbf{h}_i\, \mathbf{h}_j\beta_{ij}\right\}$$

and the thermal ellipsoids were calculated using program BADTEA written by Dr. L. W. Finger, Geophysical Laboratory. His least-squares program for site-occupancy refinement was used to obtain (Fe + Mn)/Mg site occupancies for the *C*-centered manganoan cummingtonite, fixing total chemical contents from the analysis (Klein, 1964). No large correlations between parameters were noted during any of the refinements.

The results of the five new refinements are compared with published results for three other clinoamphiboles as follows: Table 3, final positional parameters and equivalent isotropic temperature factors; Table 4[1], observed and calculated structure factors (for the new refinements only); Table 5, interatomic distances for tetrahedral chains; Table 6, interatomic angles in tetrahedral chains; Table 7, interatomic distances between oxygen atoms and the *A*- and *M*-sites with all occupancies normalized to 1.00; Table 8, selected interatomic angles for the $M(1)$, $M(2)$, $M(3)$ and A sites. The anisotropic temperature factor coefficients β for tremolite are given in Table 9, and the

---

[1] Table 4 may be ordered as NAPS Document #00455 from ASIS National Auxiliary Publications Service, c/o CCM Information Sciences, Inc., 22 West 34th St., New York, N.Y. 10001, remitting in advance $1.00 for microfiche or $3.00 for photocopies, payable to ASIS-NAPS.

TABLE 2. DATA COLLECTION INFORMATION FOR EIGHT MONOCLINIC AMPHIBOLES

	Tremolite G-21, crystal-A Present study	Cummingtonite Ghose (1961)	Grunerite Finger and Zoltai (1967)	*C*-centered manganoan cummingtonite Klein No. 2, crystal-1 Present study	Glaucophane Papike and Clark (1968)	Hornblende Present study	Potassic richterite Present study	Primitive manganoan cummingtonite USNM 115046 crystal-6 Present study
Size of crystal (mm)	0.31×0.15 ×0.22	0.20×0.20 ×0.3	0.11×0.17 ×0.34	0.21×0.18 ×0.08	0.16×0.04 ×0.03	0.06×0.08 ×0.20	0.08×0.10 ×0.50	0.09×0.04 ×0.18
Radiation/filter	Mo/Nb	Mo/crystal monochromator	Mo/Nb	Mo/Nb	Mo/Nb	Mo/Nb	Mo/Nb	Mo/Nb
Collection method	a	b	c	a	a	a	a	a
Crystal axis for data collection	c^*	c	c	c^*	c^*	$[10\bar{1}]^*$	c^*	c^*
Absorption correction	yes	no	yes	yes	yes	yes	yes	yes
μ, cm^{-1}	14.4	not given	55.5	27.9	17.8	25.8	18.3	19.1
No. of $\|F_0\|>0$	1701	1161	1198	1611	963	1052	1511	1860
Final R	0.035	.121	0.045	0.048	0.080	0.047	0.062	0.055
Standard deviation in $\|F\|$	1.91	—	—	4.00	—	4.33	4.27	3.97

[a] Normal-beam equatorial, 4-circle automatic diffractometer, scintillation counter, 2θ scan.

[b] Equiinclination Weissenberg, Geiger counter.

[c] Equiinclination Weissenberg, scintillation counter.

magnitudes and orientations of the principal axes of the thermal ellipsoids, in Table 10.

THE $C2/m$ CLINOAMPHIBOLE CRYSTAL STRUCTURE

The general features of the $C2/m$ clinoamphibole crystal structure are well known and will not be discussed here in detail. A review of the basic features may be had by referring to Figure 1. The $M(1)$, $M(2)$ and $M(3)$ octahedral sites may accommodate Mg, Al, Fe^{2+}, Fe^{3+}, Ti and Mn^{2+} and rarely other elements; these sites are too small to accommodate Na, Ca, or K. The $M(4)$ site, with distorted six- to eight-fold coordination, can accommodate either large cations such as Ca and Na or the smaller Mn^{2+} and Fe^{2+} but it is too small for K. Only limited amounts of Mg can be accommodated in the $M(4)$ site in $C2/m$ clinoamphiboles, a point that is discussed in connection with the primitive cummingtonite. The highly distorted A site may be vacant or may contain either or both Na and K, and possibly minor amounts of excess Ca. The two tetrahedral sites $T(1)$ and $T(2)$ are usually occupied by Si or Al, but may take some Fe^{3+} and Ti.

TREMOLITE

The cation sites. Ideally, the tremolite structure has no occupancy disorder. Its $M(1)$, $M(2)$ and $M(3)$ octahedral sites are filled by Mg, the $M(4)$ site, by Ca, the A site is vacant, and the tetrahedral sites $T(1)$ and $T(2)$ contain only Si. The crystal selected for structural examination contains a little tetrahedral Al, small amounts of Al^{VI}, Fe and Mn, which would presumably be distributed over the $M(1)$, $M(2)$ and $M(3)$ sites, and also a minor amount of Na (Table 1), which would be associated with Ca in $M(4)$. However, the impurities are so slight that we believed their effect on the refinement would be insignificant. Accordingly we have used the ideal model consistent with composition $Ca_2Mg_5Si_8O_{22}(OH)_2$ throughout the refinements.

The mean M-O distances for the three octahedral sites are very close in value (Table 7), 2.075 Å for $M(1)$, 2.077 Å for $M(2)$ and 2.066 Å for $M(3)$, showing that the sites are nearly identical in size when occupied by the same cation. The equivalent isotropic temperature factors (Table 3) of 0.33, 0.31 and 0.33 Å^2 for these sites, respectively, are also very similar. The coordination of Ca in the $M(4)$ site is characterized by six short bonds (2.32–2.54 Å) and two longer bonds at 2.77 Å. The mean M-O distance for $M(2)$ is identical to that found for $M(1)$ in diopside (Clark, Appleman and Papike, 1969). The two tetrahedral sites are quite distince in character (Papike and Clark, 1968), $T(1)$ being more nearly regular and $T(2)$, somewhat distorted (Table 5). These relationships hold in general for the tetrahedral sites in all the structures being considered and will be discussed in greater detail later.

The hydrogen position. Difference Fourier maps obtained during the last stages of the refinement of the tremolite structure revealed a positive region of density approximately 1 electron /Å^3 high near the expected location of

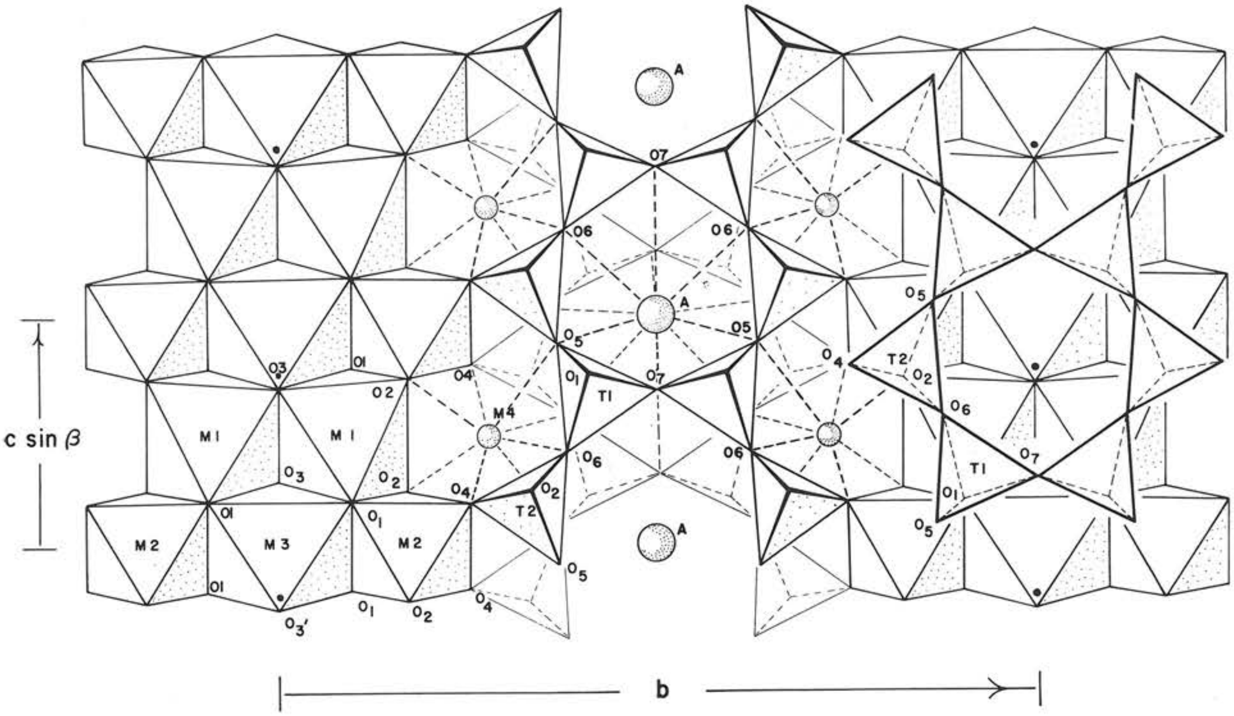

FIG. 1. Diagram of the $C2/m$ amphibole structure viewed along *a*, showing selected portions of the cell contents. The hydrogen positions are near O3 and are indicated by black dots.

the hydrogen atom. Because this peak was the largest one on the difference maps, it was assumed to arise from the contribution to the electron density by the hydrogen atom. Accordingly its position was refined and O-H distances were calculated. The parameters obtained in the last cycle are: $x = 0.199(7)$, $y = 0$, $z = 0.770(13)$ and $B = 0.5(1.2)$ Å^2. The O(3)-H distance is 0.85(7) Å and this bond, which is located in the mirror plane, makes an angle [O(3)′-O(3)-H] of 94(4)° with the octahedral strip (Fig. 1). These results seem reasonable and agree well with those of an infrared study by Burns and Strens (1966).

The anisotropic thermal model. The magnitudes and orientations of the principal axes of the thermal ellipsoids for the atoms in tremolite are presented in Table 10. The rms amplitudes vary from the low of 0.03 Å for Si to highs of 0.10 and 0.11 Å for Ca and O(7), respectively. The ellipsoids in general are not highly anisotropic. Those of the Mg atoms in sites $M(1)$, $M(2)$ and $M(3)$ are very nearly ellipsoids of revolution. The only significantly anisotropic ellipsoid is that of Ca in the $M(4)$ site; the long axis is oriented normal to *b* and at an angle of 53° with *a* and 51° with *c*. The maximum rms amplitude is thus along the direction of the long diagonal of the $M(4)$ site, and a similar orientation is found for the ellipsoid of oxygen O(4). The Ca-O(4) bond (Table 7) is the shortest one in the Ca coordination polyhedron, and the similarity in orientation of the two thermal ellipsoids reflects the coupled relationship. The ellipsoids of oxygens O(3) and O(7) each have the long axis oriented in the general direction of the vacant A site. In the tetrahedral sites, the ellipsoids of the Si atoms each have the short axis oriented towards the apical oxygens O(1) and O(2).

C-CENTERED MANGANOAN CUMMINGTONITE

The first investigators to recognize that Fe^{2+} concentrates in the $M(4)$ site of the grunerite structure were Ghose and Hellner (1959). The Fe^{2+} occupancy was confirmed by later refinements on cummingtonite (Ghose, 1961; Fischer, 1966) and grunerite (Finger and Zoltai, 1967), as well as by a spectral study (Bancroft, Burns and Maddock, 1967), in which infrared and Mössbauer results were combined to obtain the cation distributions. Bancroft, Burns and Maddock also studied a manganoan cummingtonite and found no appreciable enrichment of Fe^{2+} in the $M(4)$ site of their sample. These results suggested to them that the $M(4)$ site preference is $Mn > Fe^{2+} > Mg$. The present refinement (Table 7) shows that the $M(4)$ site is highly enriched in (Mn + Fe). The X-ray diffraction method cannot discriminate between the scattering power of Fe and Mn, and Mössbauer techniques are not applicable to Mn, but consideration of the results of both methods demonstrates that the $M(4)$ site in cummingtonites does accommodate first the large cation Mn^{2+}, then Fe^{2+}, and finally Mg. Any small amounts of Ca and perhaps Na, if present, also enter the $M(4)$ site.

Further insight into the Mn^{2+}, Fe^{2+} and Mg distribution over the *M*-sites can be gained by comparing the ob-

TABLE 3. FINAL POSITIONAL PARAMETERS AND TEMPERATURE FACTORS FOR EIGHT MONOCLINIC AMPHIBOLES

Atom[a]	Parameter[b]	Tremolite Present study	Cummingtonite Ghose (1961)	Grunerite Finger and Zoltai (1967)	*C*-centered manganoan cummingtonite Present study	Glaucophane Papike and Clark (1968)	Hornblende Present study	Potassic richterite Present study	Primitive manganoan cummingtonite[c] Present study	
									A Set	B Set
O(1)	x	0.1117(2)	0.1129(6)	0.1129(4)	0.1141(3)	0.1092(6)	0.1063(4)	0.1104(3)	0.1161(7)	0.6123(6)
	y	0.0860(1)	0.0878(3)	0.0885(2)	0.0865(2)	0.0927(3)	0.0882(2)	0.0854(2)	0.0867(3)	0.5855(4)
	z	0.2171(3)	0.2056(12)	0.2054(8)	0.2110(5)	0.2037(11)	0.2179(8)	0.2202(6)	0.2056(10)	0.2196(10)
	B	(0.35)	0.82(8)	(0.67)	(0.38)	0.50(8)	(0.77)	(0.46)	(0.30)	(0.51)
O(2)	x	0.1185(2)	0.1229(6)	0.1262(4)	0.1222(3)	0.1177(6)	0.1186(4)	0.1173(3)	0.1195(7)	0.6234(7)
	y	0.1712(1)	0.1713(3)	0.1734(2)	0.1723(2)	0.1714(3)	0.1729(2)	0.1694(2)	0.1732(3)	0.6706(3)
	z	0.7240(3)	0.7170(13)	0.7151(8)	0.7190(6)	0.7480(11)	0.7310(8)	0.7260(6)	0.7154(10)	0.7223(10)
	B	(0.39)	0.93(8)	(0.67)	(0.56)	0.50(8)	(0.79)	(0.60)	(0.40)	(0.52)
O(3)	x	0.1096(2)	0.1135(9)	0.1164(7)	0.1128(5)	0.1126(9)	0.1076(6)	0.1023(4)	0.1095(10)	0.6150(11)
	y	0	0	0	0	0	0	0	0	0
	z	0.7152(4)	0.7077(18)	0.7044(11)	0.7108(9)	0.7088(16)	0.7122(12)	0.7152(8)	0.7083(15)	0.7106(15)
	B	(0.46)	1.13(12)	(1.19)	(0.59)	0.65(12)	(1.03)	(0.34)	(0.37)	(0.58)
O(4)	x	0.3654(2)	0.3789(6)	0.3837(4)	0.3739(4)	0.3679(6)	0.3666(5)	0.3613(4)	0.3716(8)	0.8773(8)
	y	0.2480(1)	0.2465(3)	0.2414(2)	0.2473(2)	0.2529(3)	0.2505(2)	0.2483(2)	0.2482(4)	0.7472(3)
	z	0.7933(3)	0.7740(13)	0.7688(8)	0.7772(6)	0.8058(11)	0.7893(9)	0.7994(7)	0.7866(11)	0.7706(11)
	B	(0.51)	1.35(9)	(0.70)	(0.71)	0.61(8)	(1.07)	(0.94)	(0.75)	(0.58)
O(5)	x	0.3465(2)	0.3524(6)	0.3490(4)	0.3495(3)	0.3548(6)	0.3501(4)	0.3442(4)	0.3501(7)	0.8497(7)
	y	0.1343(1)	0.1312(3)	0.1277(2)	0.1305(2)	0.1318(3)	0.1392(2)	0.1300(2)	0.1262(4)	0.6359(4)
	z	0.0992(3)	0.0663(11)	0.0527(7)	0.0660(6)	0.0893(11)	0.1094(8)	0.0986(7)	0.0534(11)	0.0834(10)
	B	(0.46)	1.35(10)	(0.73)	(0.75)	0.64(8)	(1.02)	(0.82)	(0.75)	(0.45)
O(6)	x	0.3436(2)	0.3484(6)	0.3478(4)	0.3491(3)	0.3407(6)	0.3451(4)	0.3410(3)	0.3512(7)	0.8481(7)
	y	0.1185(1)	0.1185(3)	0.1176(2)	0.1214(2)	0.1224(3)	0.1175(2)	0.1176(2)	0.1243(4)	0.6182(4)
	z	0.5884(3)	0.5616(11)	0.5522(7)	0.5597(6)	0.5814(11)	0.6069(9)	0.5947(7)	0.5480(11)	0.5747(11)
	B	(0.45)	1.37(10)	(0.91)	(0.81)	0.68(8)	(1.09)	(0.76)	(0.96)	(0.81)
O(7)	x	0.3370(2)	0.3424(8)	0.3377(6)	0.3428(5)	0.3317(9)	0.3392(6)	0.3334(5)	0.3477(10)	0.8407(11)
	y	0	0	0	0	0	0	0	0	0.50
	z	0.2921(5)	0.2696(17)	0.2704(11)	0.2806(10)	0.3018(16)	0.2840(13)	0.3065(10)	0.2908(17)	0.2742(17)
	B	(0.50)	1.17(12)	(0.79)	(0.82)	0.66(11)	(1.27)	(0.67)	(0.63)	(0.78)
$T(1)$	x	0.2804(1)	0.2880(2)	0.2864(2)	0.2862(1)	0.2831(2)	0.2813(2)	0.2756(1)	0.2867(3)	0.7863(3)
	y	0.0840(1)	0.0842(1)	0.08353(9)	0.0842(1)	0.0871(1)	0.0857(1)	0.0849(1)	0.0848(1)	0.5840(1)
	z	0.2964(1)	0.2747(5)	0.2707(3)	0.2777(2)	0.2931(4)	0.3032(3)	0.3022(2)	0.2731(4)	0.2854(4)
	B	(0.19)	0.73(5)	(0.40)	(0.30)	0.31(3)	(0.49)	(0.42)	(0.34)	(0.19)
$T(2)$	x	0.2887(1)	0.2976(2)	0.2992(2)	0.2952(1)	0.2920(2)	0.2909(2)	0.2846(1)	0.2938(3)	0.7962(3)
	y	0.1711(1)	0.1687(1)	0.16673(9)	0.1700(1)	0.1730(1)	0.1728(1)	0.1718(1)	0.1708(1)	0.6697(1)
	z	0.8042(1)	0.7819(4)	0.7782(3)	0.7849(2)	0.8087(4)	0.8112(3)	0.8080(2)	0.7805(4)	0.7915(4)
	B	(0.19)	0.76(5)	(0.43)	(0.35)	0.29(3)	(0.47)	(0.37)	(0.25)	(0.35)
$M(1)$	x	0	0	0	0	0	0	0	0.0003(4)	
	y	0.0878(1)	0.0874(1)	0.08786(8)	0.0871(1)	0.0908(2)	0.0859(1)	0.0886(1)	0.0869(1)	
	z	0.50	0.50	0.50	0.50	0.50	0.50	0.50	0.4931(6)	
	B	(0.33)	1.00(5)	(0.49)	(0.45)	0.38(5)	(0.87)	(0.61)	(0.38)	
$M(2)$	x	0	0	0	0	0	0	0	0.0002(4)	
	y	0.1766(1)	0.1775(2)	0.17933(8)	0.1773(1)	0.1807(2)	0.1778(1)	0.1793(1)	0.1766(1)	
	z	0	0	0	0	0	0	0	0.9943(6)	
	B	(0.31)	0.95(6)	(0.47)	(0.39)	0.26(4)	(0.77)	(0.38)	(0.37)	
$M(3)$	x	0	0	0	0	0	0	0	0.9988(7)	
	y	0	0	0	0	0	0	0	0	
	z	0	0	0	0	0	0	0	0.9976(9)	
	B	(0.33)	0.99(6)	(0.42)	(0.27)	0.24(3)	(0.48)	(0.65)	(0.36)	
$M(4)$	x	0	0	0	0	0	0	0	0.9980(3)	
	y	0.2776(1)	0.2598(1)	0.25755(7)	0.2636(1)	0.2772(3)	0.2781(1)	0.2779(1)	0.2639(1)	
	z	0.50	0.50	0.50	0.50	0.50	0.50	0.50	0.4916(4)	
	B	(0.57)	0.84(5)	(0.84)	(0.81)	0.80(7)	(0.85)	(0.80)	(0.95)	
A	x	vacant	vacant	vacant	vacant	vacant	0.4710(17)	0.4801(7)	vacant	
	y						0	0		
	z						0.9388(24)	0.9569(11)		
	B						(5.47)	(2.09)		

[a] O(3) = O^{2-}, OH^-, F^-, Cl^-.

[b] Errors in parentheses are one standard deviation; for 0.1117(2) read 0.1117 ± 0.0002. Temperature factors ($Å^2$) in parentheses represent equivalent isotropic values from anisotropic refinements. Positions given for the *A* site represent those of a half-atom

[c] Primitive manganoan cummingtonite positional parameters have been shifted from those consistent with $P2_1/m$ by $x+1/4$, $y-1/4$, z to facilitate comparison with $C2/m$ amphiboles.

TABLE 5. INTERATOMIC DISTANCES IN TETRAHEDRAL CHAINS COMPARED FOR EIGHT MONOCLINIC AMPHIBOLES

T-O distances (Å)

	Tetrahedra occupied mainly by Si							Tetrahedra occupied by Si, Al, Fe, Ti	
	Tremolite Present study	Cummingtonite Ghose (1961)	Grunerite Finger and Zoltai (1967)	*C*-centered manganoan cummingtonite Present study	Primitive manganoan cummingtonite Present study		Glaucophane Papike and Clark (1968)	Hornblende Present study	Potassic richterite Present study
					A-chain	B-chain			
Atoms									
T(1)-O(1)	1.602(2)	1.63_1	1.626(4)	1.610(3)	1.590(7)	1.621(6)	1.618(6)	1.667(4)	1.599(3)
T(1)-O(5)	1.632(2)	1.61_9	1.631(4)	1.622(4)	1.607(7)	1.634(7)	1.616(7)	1.678(5)	1.635(4)
T(1)-O(6)	1.629(2)	1.64_2	1.622(4)	1.633(3)	1.616(6)	1.636(6)	1.621(6)	1.670(5)	1.625(4)
T(1)-O(7)	1.616(1)	1.61_9	1.613(2)	1.616(2)	1.628(4)	1.603(4)	1.611(3)	1.660(3)	1.633(2)
Average	1.620	1.62_8	1.623	1.620	1.610	1.624	1.616	1.669	1.623
					Ave. A+B	(1.617)			
T(2)-O(2)	1.616(2)	1.62_7	1.624(4)	1.618(3)	1.624(7)	1.609(7)	1.618(6)	1.641(4)	1.620(3)
T(2)-O(4)	1.586(2)	1.61_7	1.600(4)	1.594(3)	1.575(7)	1.610(7)	1.594(6)	1.606(5)	1.584(4)
T(2)-O(5)	1.653(2)	1.64_6	1.613(4)	1.634(3)	1.637(6)	1.635(6)	1.637(7)	1.650(5)	1.675(4)
T(2)-O(6)	1.672(2)	1.63_8	1.650(4)	1.655(4)	1.676(7)	1.635(7)	1.654(7)	1.661(5)	1.695(4)
Average	1.632	1.63_2	1.622	1.625	1.628	1.622	1.626	1.640	1.644
					Ave. A+B	(1.625)			
				O-O distances (Å)					
T(1) tetrahedron									
O(1)-O(5)	2.681(3)	2.65_8	2.654(5)	2.660(5)	2.634(10)	2.684(9)	2.648(8)	2.774(6)	2.706(5)
O(1)-O(6)	2.666(3)	2.67_9	2.654(6)	2.661(4)	2.647(8)	2.665(8)	2.659(7)	2.747(5)	2.688(4)
O(1)-O(7)	2.649(2)	2.67_0	2.661(6)	2.652(5)	2.664(10)	2.634(10)	2.638(8)	2.742(7)	2.653(5)
O(5)-O(6)	2.602(3)	2.66_0	2.676(5)	2.629(5)	2.617(9)	2.625(8)	2.646(9)	2.682(7)	2.639(5)
O(5)-O(7)	2.638(2)	2.63_1	2.633(5)	2.628(4)	2.598(8)	2.655(7)	2.627(7)	2.690(5)	2.603(5)
O(6)-O(7)	2.639(2)	2.65_3	2.625(5)	2.642(5)	2.615(9)	2.648(9)	2.617(8)	2.718(6)	2.599(5)
Average	2.646	2.65_8	2.650	2.645	2.629	2.652	2.639	2.726	2.648
					Ave. A+B	(2.640)			
T(2) tetrahedron									
O(2)-O(4)	2.736(2)	2.75_5	2.724(5)	2.725(5)	2.714(10)	2.752(10)	2.745(8)	2.767(6)	2.767(5)
O(2)-O(5)	2.670(3)	2.66_3	2.630(6)	2.638(4)	2.654(8)	2.628(8)	2.635(8)	2.687(5)	2.690(4)
O(2)-O(6)	2.665(3)	2.63_6	2.658(5)	2.664(5)	2.704(10)	2.615(10)	2.636(9)	2.683(6)	2.679(5)
O(4)-O(5)	2.645(2)	2.65_6	2.644(5)	2.652(5)	2.644(10)	2.649(9)	2.640(8)	2.662(6)	2.686(5)
O(4)-O(6)	2.560(2)	2.57_9	2.546(6)	2.542(5)	2.550(10)	2.534(9)	2.588(8)	2.576(6)	2.579(5)
O(5)-O(6)	2.702(3)	2.69_4	2.676(6)	2.695(5)	2.679(9)	2.709(8)	2.666(8)	2.682(7)	2.665(5)
Average	2.663	2.66_4	2.646	2.653	2.658	2.648	2.652	2.676	2.678
					Ave. A+B	(2.653)			
				Si-Si distances (Å)					
T(1)-*T*(2) [through O(6)]	3.086(2)	3.09_6	3.092(3)	3.094(3)	3.088(3)	3.075(3)	3.110(3)	3.099(2)	3.079(2)
T(1)-*T*(2) [through O(5)]	3.051(2)	3.06_2	3.066(3)	3.060(2)	3.046(3)	3.055(3)	3.003(3)	3.068(2)	3.067(2)
T(1)-*T*(1) (across mirror)	3.030(2)	3.06_3	3.073(3)	3.046(2)	3.051(3)	3.021(3)	3.090(3)	3.092(2)	3.059(2)

served mean M-O distances with M-O distances calculated by taking a linear combination, in appropriate ratios, of distances from ordered end-member structures. In our calculations we used Mn-O = 2.173 Å (johannsenite, Freed and Peacor, 1967), Fe^{2+}-O = 2.137 Å (clinoferrosilite and orthoferrosilite, Burnham, 1967 and oral comm., 1968), Mg-O = 2.077 Å for the $M(1)$ and $M(2)$ sites, based on consideration of Mg-O distances in tremolite, primitive cummingtonite and diopside (Clark, Appleman and Papike, 1969), and Mg-O = 2.070 Å for the $M(3)$ site based on tremolite and primitive cummingtonite results. Using the observed and calculated distances together with the site occupancy values (Table 7), we estimate the following (very approximate) occupancies: $M(1)$ (0.79 Mg, 0.03 Fe, 0.18 Mn); $M(2)$ (0.84 Mg, 0.12 Fe, 0.04 Mn); $M(3)$ (0.88 Mg, 0.07 Fe, 0.05 Mn); $M(4)$ (0.09 Ca, 0.01 Na, 0.03 Mg, 0.78 Mn, 0.09 Fe). Although these results should be considered only approximations they do indicate that $\mathrm{Mn} > \mathrm{Fe}$ in $M(1)$, $\mathrm{Fe} > \mathrm{Mn}$ in $M(2)$, $\mathrm{Fe} \approx \mathrm{Mn}$ in $M(3)$, and $\mathrm{Mn} >> \mathrm{Fe}$ in $M(4)$. Therefore the size arguments and the chemical contents (Table 1) confirm the entrance of Mn into the octahedral sites and indicate a nonrandom distribution of Mn in these sites.

PRIMITIVE MANGANOAN CUMMINGTONITE

Primitive manganoan cummingtonite was first identified as an exsolved phase from tremolite by Bown (1965), and since then has been identified in many metamorphic rocks (Ross, Papike and Shaw, 1969). Its unit-cell dimensions and contents are similar to those of the C-centered manganoan cummingtonite, but the primitive cummingtonite has diffraction symmetry consistent with $P2_1/m$, $P2_1$ and Pm rather than with $C2/m$, $C2$ and Cm. Refinement of the structure in the centric spacegroup $P2_1/m$ appears satisfactory and no evidence for noncentric symmetry was observed. In this new clinoamphibole structure type, instead of the 13 crystallographically distinct atomic positions found in the $C2/m$ structure type for the M cations, Si and O, there are 22 such positions in the $P2_1/m$ structure type including 14 instead of seven for oxygen atoms, and four instead of two for the tetrahedral cations. It follows that instead of one crystallographically independent tetrahedral chain in the structure there are now two, which we designate as chain A and chain B (Fig. 2). There are still only four M-sites but the symmetry restrictions for these sites have been reduced, giving atoms in these locations two new degrees of positional freedom. The four sites

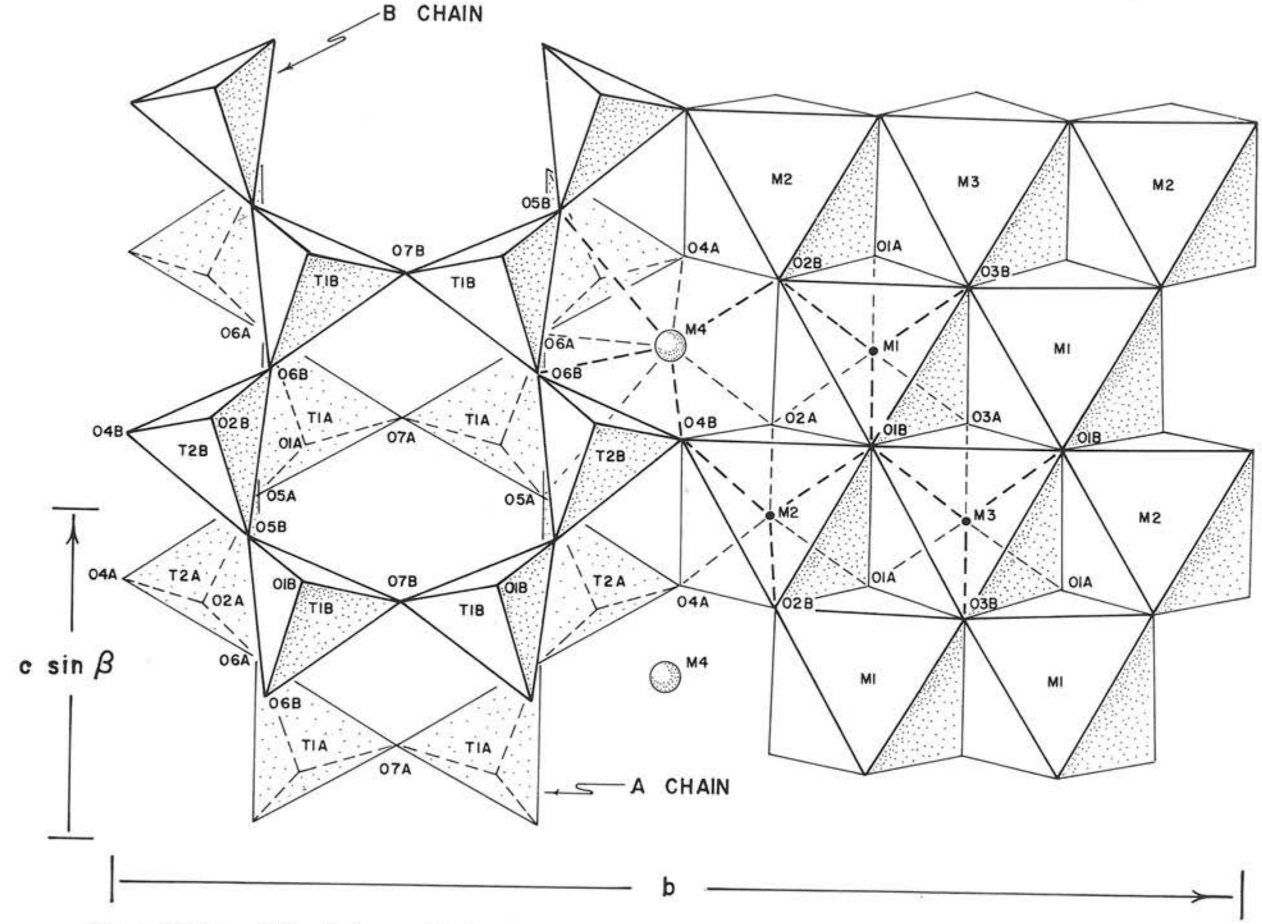

FIG. 2. Diagram of the $P2_1/m$ amphibole structure viewed along a, showing selected portions of the cell contents.

TABLE 6. INTERATOMIC ANGLES (°) IN TETRAHEDRAL CHAINS COMPARED FOR EIGHT MONOCLINIC AMPHIBOLES

Atoms	Tetrahedra occupied mainly by Si							Tetrahedra occupied by Si, Al, Fe, Ti	
	Tremolite Present study	Cummingtonite Ghose (1961)	Grunerite Finger and Zoltai (1967)	*C*-Centered manganoan cummingtonite Present study	Primitive manganoan cummingtonite Present study		Glaucophane Papike and Clark (1968)	Hornblende Present study	Potassic richterite Present study
					A chain	B chain			
O(1)-*T*(1)-O(5)	111.9(1)	109.8	109.1(2)	110.8(2)	110.9(3)	111.0(3)	110.0(3)	112.0(2)	113.6(2)
O(1)-*T*(1)-O(6)	111.1(1)	109.9	109.6(2)	110.3(2)	111.2(4)	109.7(4)	110.4(3)	110.7(2)	112.9(2)
O(1)-T(1)-O(7)	110.7(1)	110.5	110.5(3)	110.6(2)	111.7(4)	109.5(4)	109.6(4)	110.9(3)	110.3(2)
O(5)-*T*(1)-O(6)	105.8(1)	109.3	110.7(2)	107.8(2)	108.6(4)	106.7(3)	109.7(3)	106.4(2)	108.1(2)
O(5)-*T*(1)-O(7)	108.5(1)	108.6	108.5(3)	108.5(2)	106.8(4)	110.2(4)	109.0(4)	107.4(3)	105.6(2)
O(6)-*T*(1)-O(7)	108.7(1)	108.8	108.5(3)	108.9(2)	107.4(4)	109.7(4)	108.2(4)	109.3(3)	105.8(2)
Average	109.4	109.5	109.5	109.5	109.4	109.5	109.5	109.4	109.4
O(2)-*T*(2)-O(4)	117.3(1)	116.3	115.3(2)	116.0(2)	116.0(4)	117.4(4)	117.5(3)	116.8(2)	119.4(2)
O(2)-*T*(2)-O(5)	109.4(1)	109.0	108.6(2)	108.4(2)	108.8(3)	108.2(3)	108.1(3)	109.3(2)	109.4(2)
O(2)-*T*(2)-O(6)	108.2(1)	107.7	108.6(2)	109.0(2)	110.0(3)	107.4(3)	107.4(3)	108.6(2)	107.8(2)
O(4)-*T*(2)-O(5)	109.4(1)	109.0	110.8(2)	110.4(2)	110.7(3)	109.4(3)	109.6(3)	109.6(2)	110.9(2)
O(4)-*T*(2)-O(6)	103.5(1)	104.7	103.2(2)	102.9(2)	103.2(4)	102.6(4)	105.6(3)	104.0(3)	103.6(2)
O(5)-*T*(2)-O(6)	108.6(1)	110.3	110.2(2)	110.0(2)	107.8(4)	111.9(3)	108.2(3)	108.1(2)	104.4(2)
Average	109.4	109.5	109.4	109.4	109.4	109.5	109.4	109.4	109.3
T(1)-O(5)-*T*(2)	136.5(1)	139.4	141.9(3)	140.0(2)	139.8(5)	138.4(4)	134.7(4)	134.4(3)	135.8(2)
T(1)-O(6)-*T*(2)	138.4(1)	141.4	141.9(2)	140.4(2)	139.4(4)	140.2(4)	143.5(4)	137.0(3)	136.1(2)
T(1)-O(7)-*T*(1)	139.3(2)	142.2	144.6(4)	141.0(3)	139.1(6)	141.0(7)	147.2(6)	137.3(4)	139.0(4)
O(5)-O(6)-O(5)	167.6(1)	170.0	172.0(3)	172.9(2)	178.4(4)	166.2(4)	170.8(3)	163.1(2)	170.2(2)
					Ave. A+B (172.3)				
O(5)-O(7)-O(6) (across mirror)	166.9(2)	168.7	171.1(3)	171.8(2)	177.5(5)	165.9(4)	170.3(3)	161.8(3)	169.6(2)

are no longer on two-fold axes, although $M(3)$ does remain on a mirror plane.

A detailed comparison of interatomic distances and angles for the primitive and *C*-centered manganoan cummingtonites shows that the "average structure" of the primitive amphibole is, as would be expected, close to the structure of the *C*-centered amphibole. In fact, when the primitive structure is treated as *C*-centered by eliminating from refinement the approximately 500 reflections violating that symmetry, the refinement yields positional parameters identical (within 2 standard deviations) to those obtained for the *C*-centered manganoan cummingtonite.

In comparing the two structures, we find that the differences between the O(5)-O(6)-O(5) angles of the tetrahedral chains are significant. For *C*-centered manganoan cummingtonite this angle is 173°, while in primitive cummingtonite, chain A is straighter with an angle of 178° and chain B is relatively more kinked with an angle of 166°, similar to that observed in tremolite (Table 6). The geometry of the relative chain distortions and of the $M(4)$ site resembles that of anthophyllite. The occupancy of the $M(4)$ site is critical and appears to be the key to understanding the existence of the $P2_1/m$ structure and some of the phase relations in the amphibole quadrilateral (Ross, Papike and Weiblen, 1968). Both the large Ca and smaller Mg cations must be accommodated in this site due to the chemical composition (Table 7); the presence of the Mg in $M(4)$ is critical. With $C2/m$ symmetry the tetrahedral chains are equivalent and cannot distort independently, whereas in $P2_1/m$ they can and do, in order to provide the necessary coordination for the joint Ca/Mg occupancy. The $M(1)$, $M(2)$ and $M(3)$ sites are virtually filled by Mg in the primitive structure, according to our refinement and the results of an infrared spectral study (R. W. T. Wilkins, written comm., 1968).

The structure of orthorhombic anthophyllite may be considered as made up of blocks of the primitive cummingtonite structure stacked in an ABAB sequence, where A and B have the *a* unit-cell repeat and B is related to A by approximately 180° rotation around a^*. The stacking sequence cannot be described in terms of a twinning operation because the two structure types have significant differences unrelated to stacking sequence variations. The $P2_1/m$ structure is the closest known to that of anthophyllite that can be produced from a $C2/m$ amphibole without breaking bonds. Therefore, if the $C2/m$ structure is stable at high temperatures and the orthorhombic anthophyllite is stable at low temperatures, the $P2_1/m$ phase may be a metastable intermediate phase. Crystals subjected to high temperatures are now being studied to check this hypothesis. The relationship of $P2_1/m$ and $C2/m$ amphiboles is discussed further by Ross, Papike and Shaw (1969), and amphibole-pyroxene analogies are described at the close of the present paper.

Potassic and Aluminous Hornblende

In 1966 Brian Mason published a paper entitled "Pyrope, augite and hornblende from Kakanui, New Zealand." These minerals occur as xenocrysts in a volcanic breccia, and Mason suggests that they may have originated in the lower crust or upper mantle. The occurrence of potassic hornblendes in the upper mantle, similar to those described by Mason, was predicted by Oxburgh (1964) to explain observed potassium abundances in basaltic rocks. Because of the petrologic significance of this hornblende, special attention during the structural refinement was given to the crystal-chemical behavior of potassium and aluminum.

Distribution of tetrahedral aluminum. The Kakanui hornblende has approximately two tetrahedral Al atoms per formula unit and so is ideally suited for study of the distribution of Al between the two crystallographically and energetically distinct tetrahedral sites $T(1)$ and $T(2)$. To determine this distribution we resort mainly to the size considerations developed by Smith (1954) and discussed by Smith and Bailey (1963). However, estimation of the distribution can be arrived at in several ways.

First, an average of all T-O distances in each of a number of structures can be used to establish a Smith-Bailey plot for amphiboles. Second, the two tetrahedra can be considered separately with respect to size, by examining average $T(1)$-O and $T(2)$-O values. Third, because $T(1)$ is fairly regular tetrahedron, the $T(1)$-O average can be retained but within $T(2)$ only the short nonbridging $T(2)$-O(2) and $T(2)$-O(4) distances are used to obtain an average. This third method takes into account the individual distortions in each tetrahedron as well as the overall size differences. Because the chemical species in the $M(4)$ site contributes to the distortions observed in $T(2)$, the Si-O values in tremolite, which has Ca in $M(4)$, are used in applying the second and third methods to hornblende.

Using the first method, the curve is established from a mean Si-O distance of 1.623 Å, averaged over the values given in Table 5 for Si-occupied tetrahedra (excluding cummingtonite), and a mean T-O distance of 1.654 Å from the hornblende data (Table 5) for a tetrahedron containing 25 percent Al. Application of this curve to the individual tetrahedra in hornblende gives the occupancies (0.37 Al, 0.63 Si) for $T(1)$ and (0.13 Al, 0.87 Si) for $T(2)$. However, this method is probably less reliable because it does not take into account the differences in size and distortions that occur between $T(1)$ and $T(2)$ even when both are entirely occupied by Si. Using the second method the mean value of 1.669 Å for $T(1)$ in hornblende is compared with the value 1.620 Å for a pure Si tetrahedron in tremolite, and the mean value of 1.640 Å for $T(2)$ in hornblende, with the value 1.632 Å in tremolite. These values are used with the chemical data for hornblende to allot aluminum. This approach yields the occupancies (0.43 Al, 0.57 Si) in $T(1)$ and (0.07 Al, 0.93 Si) in $T(2)$. In the third method the value of 1.624 Å for mean T-O distance to nonbridging oxygens, O(2) and O(4), in hornblende is compared with the mean T-O distance of 1.601 Å to nonbridging oxygens in tremolite. The following occupancies are obtained: for $T(1)$ (0.34 Al, 0.66 Si), for $T(2)$ (0.16 Al, 0.84 Si). Obviously, the errors in these estimates are large, but the $T(1)$ tetrahedron in this hornblende is clearly enriched in aluminum relative to $T(2)$, in accord with the prediction by DeVore (1957). The significance of this observation is discussed in the section on General Structural Features of Clinoamphiboles.

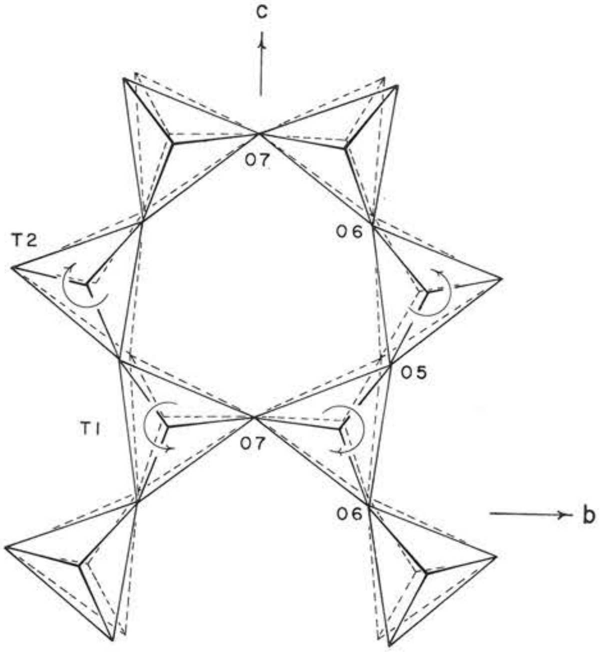

Fig. 3. Diagram of the double chains of tetrahedra in glaucophane and hornblende. Dashed lines represent glaucophane chains and solid lines represent hornblende chains. Arrows indicate the relative directions of rotation.

The size and distortions in the $T(2)$ tetrahedron of hornblende are very similar to those for the tetrahedron of an aluminous augite (Clark, Appleman and Papike, 1969). The mean T-O distance is 1.640 Å in both structures. The chemistry of the augite is compatible with an occupancy of (0.08 Al, 0.92 Si) in its tetrahedral site and, if similar T-O distances do reflect the site occupancy, the $T(2)$ tetrahedron in hornblende should also have (0.08 Al, 0.92 Si). Essentially those values were obtained by the second method for estimating the hornblende tetrahedral site contents. This agreement may indicate that provisionally the second method is best to use until we have more data on amphiboles containing tetrahedral aluminum.

The tetrahedral chains of hornblende are kinked relative

TABLE 7. INTERATOMIC DISTANCES Å FOR OXYGEN ATOMS AND THE A, $M(1)$, $M(2)$, $M(3)$ AND $M(4)$ SITES COMPARDE FOR EIGHT MONOCLINIC AMPHIBOLES

Atoms	Tremolite Present study[a]			Cummingtonite Fischer (1966)		Cummingtonite Calculated from Ghose (1961)	Grunerite Finger and Zoltai (1967)			C-centered Manganoan Cummingtonite Present study[b]			Primitive Manganoan Cummingtonite Present study[c]		Distance	
	Site occupancy	Bond multiplicity	Distance	Site occupancy	Bond multiplicity	Distance	Site occupancy	Bond multiplicity	Distance	Site occupancy	Bond multiplicity	Distance	Site occupancy	Bond multiplicity	A-set	B-set
A-O(5)	Vacant	4	2.970(2)	Vacant	4	2.828	Vacant	4	2.802(4)	Vacant	4	2.828(3)	Vacant	2	2.733(7)	2.919(7)
A-O(6)		4	3.156(2)		4	3.285		4	3.328(4)		4	3.303(3)		2	3.357(7)	3.206(6)
A-O(7)		2	2.486(3)		2	2.280		2	2.327(6)		2	2.340(6)		1	2.339(10)	2.322(11),
		2	3.672(3)		2	3.872		2	3.885(6)		2	3.791(6)		1	3.720(8)	3.813(9)
mean for 12			3.068			3.063			3.079			3.066			3.052	
mean for 8			—			—			—			—			—	
$M(1)$-O(1)	1.0 Mg	2	2.064(2)	0.16 Fe 0.84 Mg	2	2.076	0.854(9) Fe 0.146 Mg	2	2.083(5)	0.208(9) Fe+Mn 0.792 Mg	2	2.071(3)	1.0 Mg	1	2.069(7)	2.047(7)
$M(1)$-O(2)		2	2.078(2)		2	2.115		2	2.164(4)		2	2.124(3)		1	2.123(6)	2.093(6)
$M(1)$-O(3)		2	2.083(2)		2	2.103		2	2.131(4)		2	2.092(3)		1	2.077(6)	2.075(6)
mean for 6			2.075			2.098			2.126			2.096			2.082	
$M(2)$-O(1)	1.0 Mg	2	2.133(2)	0.05 Fe 0.95 Mg	2	2.128	0.775(9) Fe 0.225 Mg	2	2.162(4)	0.158(8) Fe+Mn 0.842 Mg	2	2.148(3)	1.0 Mg	1	2.134(6)	2.143(6)
$M(2)$-O(2)		2	2.083(2)		2	2.093		2	2.130(4)		2	2.092(3)		1	2.055(7)	2.106(8)
$M(2)$-O(4)		2	2.014(2)		2	2.029		2	2.078(4)		2	2.024(3)		1	2.014(7)	2.013(6)
mean for 6			2.077			2.083			2.123			2.088			2.078	
$M(3)$-O(1)	1.0 Mg	4	2.070(2)	0.16 Fe 0.84 Mg	4	2.102	0.865(14) Fe 0.135 Mg	4	2.128(4)	0.125(14) Fe+Mn 0.875 Mg	4	2.089(3)	1.0 Mg	2	2.090(6)	2.070(7)
$M(3)$-O(3)		2	2.057(3)		2	2.070		2	2.110(6)		2	2.063(5)		1	2.043(11)	2.076(11)
mean for 6			2.066			2.091			2.122			2.080			2.073	
$M(4)$-O(2)	0.95 Ca 0.05 Na	2	2.397(2)	0.87 Fe 0.13 Mg	2	2.176	0.988(12) Fe 0.012 Mg	2	2.144(4)	0.88 Mn+Fe 0.03 Mg 0.09 Ca	2	2.204(3)	0.01 Fe 0.49 Mn 0.28 Mg 0.19 Ca 0.03 Na	1	2.195(6)	2.208(6)
$M(4)$-O(4)		2	2.321(2)		2	2.041		2	1.988(4)		2	2.109(4)		1	2.139(8)	2.074(8)
$M(4)$-O(6)		2	2.539(2)		2	2.699		2	2.764(5)		2	2.592(4)		1	2.511(8)	2.650(8)
$M(4)$-O(5)		2	2.767(2)		2	3.147		2	3.290(4)		2	3.101(3)		1	3.209(6)	2.932(6)
mean for 6			2.419			2.305			2.299			2.302			2.296	
mean for 8			2.506			2.516			2.546			2.502			2.490	
															z	$(1-z)$
$M(1)$-$M(1)$			3.169(2)			3.179			3.232(3)			3.151(3)			3.129(3)	
$M(1)$-$M(2)$			3.086(2)			3.130			3.155(1)			3.118(2)			3.108(4)	3.097(4)
$M(1)$-$M(3)$			3.077(1)			3.104			3.120(1)			3.089(2)			3.100(5)	3.054(5)
$M(1)$-$M(4)$			3.423(2)			3.136			3.121(2)			3.191(2)			3.183(2)	
$M(2)$-$M(3)$			3.187(2)			3.228			3.298(1)			3.207(2)			3.180(2)	
$M(2)$-$M(4)$			3.204(1)			3.058			3.032(1)			3.080(2)			3.085(3)	3.069(3)

[a] A small amount of Fe+Mn is present in the $M(1)$, $M(2)$, and $M(3)$ sites. The $M(4)$ site occupancy was derived from the chemical analysis.

[b] In the site occupancy refinement, Mn and Fe were necessarily combined, but it is believed the $M(4)$ site contains most of the Mn (see text).

[c] No site occupancy refinement was done, but infrared spectral studies and isotropic temperature factors indicate that the $M(1)$, $M(2)$, and $M(3)$ sites are essentially completely occupied by Mg (see text).

TABLE 7.—(*Continued*)

Atoms	Glaucophane Papike and Clark (1968)			Hornblende[d] Present study					Potassic richterite[e] Present study				
	Site occupancy	Bond multi-plicity	Distance	Site occupancy	Bond multi-plicity	Distance[f]	Bond multi-plicity	Distance[g]	Site occupancy	Bond Multi-plicity	Distance[f]	Bond multi-plicity	Distance[g]
A-O(5)	Vacant	4	2.814(6)	0.6 Na 0.4 K	4	3.049(5)	2 2	3.022(11) 3.121(11)	1.0 K	4	2.937(4)	2 2	2.905(6) 2.992(6)
A-O(6)		4	3.216(5)		4	3.086(4)	2 2	2.829(9) 3.364(10)		4	3.139(4)	2 2	2.954(5) 3.336(6)
A-O(7)		2	2.519(10)		2	2.459(8)	1 1	2.464(19) 2.510(18)		2	2.610(6)	1 1	2.603(9) 2.642(9)
		2	3.666(8)		2	3.714(7)	1 1	3.376(14) 4.059(14)		2	3.614(5)	1 1	3.372(7) 3.859(8)
mean for 12			3.041			3.074		3.090			3.063		3.071
mean for 8			—			—		2.865			—		2.868
M(1)-O(1)	0.16 Fe 0.84 Mg	2	2.078(6)	0.271 Fe 0.557 Mg 0.096 Ti 0.076 Al	2	2.042(5)			0.057 Fe 0.907 Mg 0.034 Ti 0.002 Mn	2	2.064(4)		
M(1)-O(2)		2	2.082(6)		2	2.141(4)				2	2.051(4)		
M(1)-O(3)		2	2.100(5)		2	2.043(4)				2	2.071(3)		
mean for 6			2.087			2.075					2.062		
M(2)-O(1)	0.09 Fe 0.91 Al	2	2.038(6)	0.271 Fe 0.557 Mg 0.096 Ti 0.076 Al	2	2.101(4)			0.057 Fe 0.907 Mg 0.034 Ti 0.002 Mn	2	2.187(4)		
M(2)-O(2)		2	1.943(6)		2	2.072(5)				2	2.095(4)		
M(2)-O(4)		2	1.849(6)		2	1.973(4)				2	2.000(4)		
mean for 6			1.943			2.049					2.094		
M(3)-O(1)	0.29 Fe 0.71 Mg	4	2.103(5)	0.271 Fe 0.557 Mg 0.096 Ti 0.076 Al	4	2.083(4)			0.057 Fe 0.907 Mg 0.034 Ti 0.002 Mn	4	2.070(3)		
M(3)-O(3)		2	2.077(5)		2	2.076(7)				2	2.028(5)		
mean for 6			2.094			2.081					2.056		
M(4)-O(2)	0.98 Na 0.02 Ca	2	2.411(6)	0.815 Ca 0.130 Na 0.055 (Fe, Mg, Ti and Al)	2	2.394(4)			0.50 Ca 0.50 Na	2	2.431(4)		
M(4)-O(4)		2	2.337(6)		2	2.328(5)				2	2.407(4)		
M(4)-O(6)		2	2.446(6)		2	2.582(5)				2	2.599(4)		
M(4)-O(5)		2	2.798(6)		2	2.665(4)				2	2.825(4)		
mean for 6			2.398			2.435					2.479		
mean for 8			2.498			2.492					2.565		
M(1)-M(1)			3.221(4)			3.103(3)					3.193(4)		
M(1)-M(2)			3.091(2)			3.129(2)					3.109(2)		
M(1)-M(3)			3.099(2)			3.074(1)					3.088(2)		
M(1)-M(4)			3.307(6)			3.468(3)					3.410(3)		
M(2)-M(3)			3.206(3)			3.210(2)					3.233(2)		
M(2)-M(4)			3.153(3)			3.211(2)					3.182(2)		

[d] No site occupancy refinement was done and the octahedral cations were assumed to be disordered. There is an indication based on bond distances and temperature factors, however, that M(2) is enriched in the smaller octahedral cations Al, Fe^{3+}, and perhaps Ti, and the M(3) site is enriched in Fe (see text).

[e] No site occupancy refinement was done and the octahedral cations were assumed to be disordered. There is an indication based on bond distances and temperature factors, however, that the M(2) site may be enriched in Fe^{2+} relative to M(1) and M(3) (see text).

[f] AO distances calculated for atom assumed to be at 1/2, 0, 0.

[g] A-O distances calculated for atom displaced from 1/2, 0, 0 (half-atom, see Table 3).

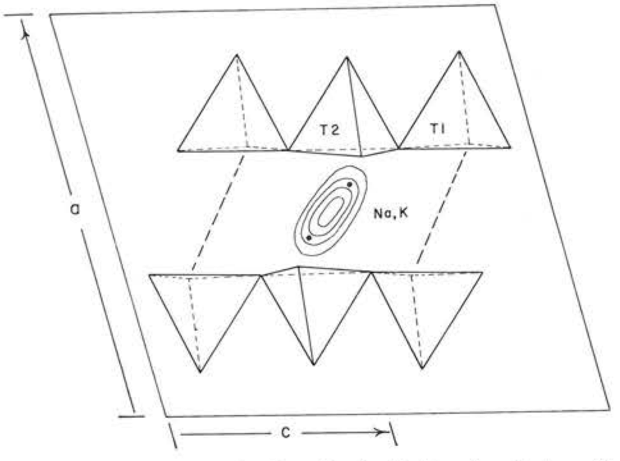

FIG. 4. Diagram of the hornblende *A* site viewed along *b*. The contour lines (contour interval 4 electrons / Å^3) represent the (Na, K) contribution to the electron density. Black dots mark the "split-atom" positions for (Na, K).

to the chains in glaucophane; the O(5)-O(6)-O(5) angle in hornblende is 163.1°, compared to 170.8° in glaucophane (Table 6), a difference of 7.7°. Tetrahedral rotation of this type was predicted by Ghose (1965) and is illustrated in Figure 3. Such rotation tends to equalize the *c*-dimensions of the respective unit cells so that, despite significantly larger tetrahedra in hornblende (Table 5), the *c*-axes of glaucophane and hornblende differ in length by only 0.02 Å (Table 1).

The M sites. No site occupancy refinements were made for the hornblende, and cation contents were assigned to each site (Table 7) on the basis of the values from the chemical analysis (Table 1), using known cation sizes. The $M(1)$, $M(2)$ and $M(3)$ sites were assumed to be filled by the octahedral-type cations, equally divided among the three sites. The slight excess of these cations was allocated to the $M(4)$ site, together with all the Ca and enough Na to fill $M(4)$. As the overall least-squares refinement proceeded, there appeared some indications from the slightly lower average $M(2)$-O distance (2.049 Å, Table 7) and the lower isotropic temperature factor of $M(3)$ (0.48 Å^2, Table 3) that $M(2)$ is enriched in the smaller cations, $\mathrm{Al}^{\mathrm{VI}}$, Fe^{3+}, and possibly Ti, and that $M(3)$ is enriched in Fe. The mean *M-O* distance for $M(1)$ indicates that it is occupied mostly by Mg. However, no further calculations were carried out to test these indications.

Sodium and potassium in the A site. The electron density contributed by the sodium and potassium atoms in the *A* site is illustrated in Figure 4. The contour interval is four electrons/Å^3, and this elongated region of electron density can be interpreted in terms of either thermal or positional disorder of the potassium and sodium atoms. In the refinement of the structure a composite (Na, K) atom was taken to be two half-atoms, slightly separated in positions but confined to the mirror plane. This simple model is only an approximation because it does not take into account the differences between Na and K. There is some indication from the electron density along *b* that in fact Na and K are occupying slightly different locations in the *A* site. There are good crystal-chemical reasons for such behavior, and some of these are discussed in the section on General Structural Features of Clinoamphiboles.

However, if a composite (Na, K) atom is assumed to be occupying one of the two positions marked with black dots on Figure 4, the coordination can be calculated for a split-atom model (Table 7) and compared with that for an atom at the center of the *A* site (1/2, 0, 0). For the split-atom model we find eight oxygens at less than 3.1 Å with a mean distance of 2.865 Å. For the central location, we find ten oxygens at less than 3.1 Å with a mean distance of 2.946 Å. Both models appear reasonable, but by analogy with the potassic richterite, to be discussed later, the split-atom model is favored.

Potassium in hornblendes and pyroxenes. Hornblende has a crystallographic site in its structure which can accommodate potassium, but there is no analogous site in the pyroxene structure. Therefore, great caution should be used in the interpretation of analytical results suggesting high potassium content in pyroxenes. Although such pyroxenes may appear to be optically homogeneous, they are frequently found to contain fine intergrowths of amphiboles when crystals are examined by single-crystal X-ray diffraction methods. Important examples of such intergrowths identified by us in this way include jadeites from the glaucophane schists of California, augites from the Sierra Nevada batholith and from kaersutite-bearing peridotite, San Carlos, Arizona, and omphacites from the Roberts Victor eclogites, South Africa. Before relying on K/Ar dates for pyroxenes even when such dates appear reasonable, or on other quantitative work on potassium abundances in pyroxenes, these phases should be studied by single-crystal, X-ray diffraction techniques to confirm their homogeneity.

The significance of these amphibole intergrowths associated with pyroxenes supposed to contain potassium is not easy to ascertain. Various possibilities can be considered. First, the amphibole may have formed as a later alteration of the pyroxene with introduction of potassium during the alteration. Second, the amphibole could be a primary epitaxial intergrowth; third, the pyroxene could have formed from an amphibole precursor. Finally, the amphibole could have exsolved from a pyroxene host because finite solid solution between pyroxene and amphibole at high temperatures and pressures is a possibility that cannot be ignored. Crystal-chemical considerations indicate that hornblende is a suitable phase to accommodate potassium at depth in the earth, and the coordination and charge requirements of potassium may explain the retention of tetrahedral aluminum in this phase at high pressures.

POTASSIC RICHTERITE

The most potassic amphiboles reported (4.4 to 6.5% K_2O) are richterites, examples of which occur in potassic volcanics, West Kimberly, Western Australia (Prider, 1939) and in volcanic rocks, Leucite Hills, Wyoming (Carmichael, 1967). Such potassium concentrations suggest that the amphibole *A* site is filled with potassium (Table 1), and indeed the presence of the potassium is reflected in the 10.019 Å value for the *a* unit-cell dimension, which to our knowledge is the longest reported for any clinoamphibole. Crystals of this richterite display diffraction symmetry *2/m C-/-*, consistent with the centric space group *C2/m* and noncentric space groups *C2* and *Cm*. No evidence for a noncentric nature of this material was obtained from piezoelectric measurements, statistical evaluations of X-ray diffraction data, or numerous attempts at refinement of noncentric structure models. Therefore the structure reported here is the one consistent with *C2/m* symmetry.

The M sites. No site occupancy refinements were made for the potassic richterite, and cation contents were assigned, as in hornblende, on the basis of chemical analysis and crystal-chemical considerations. All Na and Ca were assigned to *M*(4), and an interesting feature of this structure is the 1:1 ratio of Na to Ca in this site. The smaller octahedral cations were divided equally among the *M*(1), *M*(2), and *M*(3) sites. There is an indication, however, based on bond distances and temperature factors that *M*(2) may be enriched in Fe^{2+} relative to *M*(1) and *M*(3).

Coordination of potassium in the A site. Electron-density sections through the *A* site revealed a highly anisotropic electron density contributed by the potassium atom. The interpretations are the same as those already given for the potassic hornblende, namely, either thermal or positional disorder. A structural model with K at the central point of the *A* site was tested but proved to be unsatisfactory in several respects. The oxygen coordination of potassium was not reasonable, the isotropic temperature factor was high at 4.5 Å², and the difference Fourier maps showed unusually large positive regions near the central location. The situation was not significantly improved by anisotropic temperature refinement.

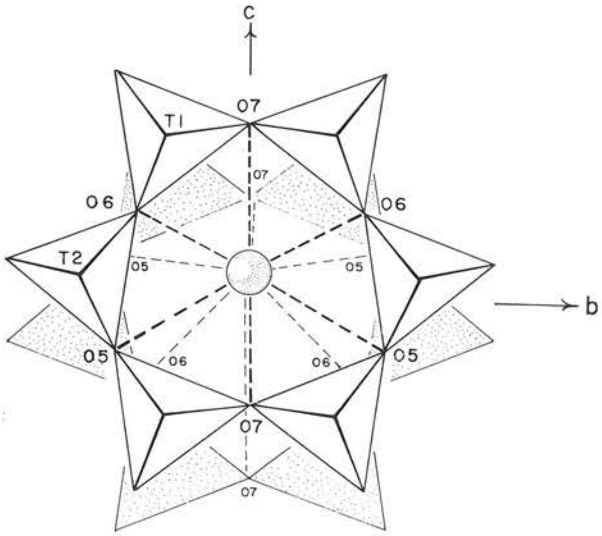

FIG. 5. Diagram of the clinoamphiboles *A* site viewed down *a* sin *β*; dashed lines show the *A*-O coordination (Table 7).

Accordingly, a structural model assuming half-atoms located at positions indicated by examination of the difference Fourier maps was tested and refined. This model gave satisfactory K-O distances, an isotropic temperature factor of 1.6 Å², which is a reasonable value for potassium in silicates, and the featureless difference maps revealed good agreement of the model with the observed data. The coordination of potassium in this half-atom position of the structure is best described as eight short bonds (less than 3.00 Å) and three long ones (Table 7, Fig. 5). The mean for the eleven distances is 2.999 Å. This value can be compared with those in other structures, as follows: the mean K-O distance for the nine closest oxygens to K in K-feldspar, 2.962 Å (Spencer B, Colville and Ribbe, 1968); the mean K-O distance for the twelve nearest oxygens to K in phengite, 3.103 Å, and in muscovite, 3.108 Å (Güven, 1968), in *3T* muscovite, 3.129 Å (Güven and Burnham, 1967), and in a synthetic lithium fluormica, 3.136 Å (Takeda and Donnay, 1966). Of particular significance, however, is the observation that according to this half-atom model richterite has eight oxygens 3.00 Å or closer to K, the mean K-O distance for eight being 2.868 Å. In the micas only six oxygens are 3.00 Å or less from K. The mean of the six K-O distances is 2.855 Å in muscovite, 2.868 Å in *3T* muscovite, 2.970 Å in phengite, and 2.995 Å in synthetic lithium fluormica. The coordination of potassium in the clinoamphibole structure is therefore tighter than in the mica structure, and this feature may be relevant to discussions concerning the relative stability of clinoamphiboles and micas in the high-pressure environment of the upper mantle.

Sodium-potassium exchange. Na ⇄ K exchange has been accomplished in feldspars and micas, providing examples of three-dimensional exchange through framework structures and two-dimensional exchange through layer structures. Clinoamphiboles have channelways running parallel to *c*, through the *A* sites (*cf.* Fig. 2*b*, Papike and Clark, 1968), and thus provide the possibility of one-dimensional exchange paths through the chain structure. Such exchange has proved feasible (Papike, Clark and Huebner, 1968), and work now in progress by Huebner and Papike demonstrates that potassic richterite [$K(NaCa)Mg_5$] and sodic richterite [$Na(NaCa)Mg_5$] can be readily synthesized and exchanged both ways. Intermediate compositions have also been obtained by exchange, direct synthesis from oxide

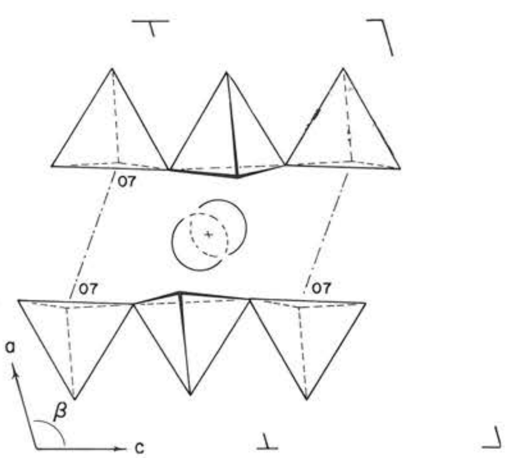

FIG. 6. Diagram of the potassic richterite A site viewed down b. The half-atom interpretation of the electron density is illustrated and the A site central point (½, 0, 0) is marked with a cross.

mixes, and homogenization starting with "end-member" amphiboles.

The changes in the unit-cell parameters (Papike, Clark and Huebner, 1968) are readily explained on a structural basis (Fig. 6). As potassium substitutes for sodium in the amphibole A site, the double chains are moved apart, increasing the length of the a axis. Substitution of K for Na also makes the geometry of the A site more regular, because a relative displacement of the six-membered rings occurs, producing an increase in β.

These results also support the suggestion that significant amounts of potassium can be accommodated in the amphibole structure under conditions similar to those prevailing in the upper mantle. In addition they show that caution should prevail in predicting the amount of amphibole in the upper mantle from observed K/Na ratios in amphiboles, because such ratios could have been changed drastically through cation exchange.

GENERAL STRUCTURAL FEATURES OF CLINOAMPHIBOLES

The $M(1)$, $M(2)$ and $M(3)$ octahedral sites. The $M(2)$ octahedron consists of six oxygen atoms, whereas $M(1)$ and $M(3)$ both have four oxygens and two (OH, F, Cl) ions (O(3), Fig. 1). The three octahedral sites are occupied mainly by (Mg + Fe) in the clinoamphibole structures compared here (Tables 7, 8). The C-centered manganoan cummingtonite has some Mn in these sites, and glaucophane has (Al + Fe) in $M2$.

In general the angles subtending shared edges of the octahedra are less than 90°, the smallest angle in all the structures except glaucophane being the $\mathrm{O(1)^u\text{-}}M\mathrm{(2)\text{-}O(1)^d}$ angle associated with the $\mathrm{O(1)^u\text{-}O(1)^d}$ edge shared between $M(2)$ and $M(3)$ (Fig. 1; u means "up", d, "down" along a). This angle is close to 80° in all eight clinoamphiboles. The largest angles in the octahedra are usually about 97 to 99°, the maximum often being for the $\mathrm{O(1)^u\text{-}}M\mathrm{(3)\text{-}O(1)^u}$ angle which reaches a high of 102.9(2)° in glaucophane (Fig. 1, Table 8). Comparison of the Mg octahedra in tremolite and in diopside (Clark, Appleman and Papike, 1969) shows that the octahedra are similar but are slightly more distorted in the amphibole structure, probably because of the increase in edge-sharing that occurs. The glaucophane $M(2)$ octahedron is also somewhat more distorted than are the Al octahedra in spodumene and jadeite.

The $M(4)$ site. The size of the cation occupying the $M(4)$ site is largely responsible for the amphibole structure type that is found. When the $M(4)$ site is occupied by Ca, Na, and/or Fe the symmetry observed is $C2/m$. When the $M(4)$ site is partially occupied by Mg the symmetry may change to $P2_1/m$, and with further enrichment of Mg in this site the amphibole may assume the orthorhombic $Pnma$ structure.

The $M(2)$ site in clinopyroxenes is directly comparable to the $M(4)$ site in clinoamphiboles, and the analogies between amphiboles and pyroxenes are striking. The $C2/c$ pyroxene structure is found when either Ca or Na occupies the $M(2)$ site; some mixture of Ca/Na is tolerated but a 1:1 ratio may be associated with the $P2$ structure type if appreciable octahedral Al is present (Clark and Papike, 1968). The occurrence of large amounts of Fe in $M(2)$ (clinopyroxene) may lead to either $P2_1/c$ pigeonite or $Pbca$ orthopyroxene, whereas the presence of Fe in $M(4)$ (amphiboles) is apparently tolerated without change in the $C2/m$ symmetry. The primitive cummingtonite is the amphibole analog of pigeonite (Papike, Ross and Clark, 1968), but it appears that the presence of appreciable amounts of Mg in $M(4)$ is necessary to produce the primitive clinoamphibole structure.

In tremolite and hornblende, $M(4)$ contains chiefly Ca. In potassic richterite, $M(4)$ has 50 percent Ca and 50 percent Na, and in glaucophane the site is filled with Na. In all these cases the coordination (Table 7) can be described as divided into six short bonds (2.32 to 2.60 Å) and two longer bonds (2.66 to 2.82 Å), exactly analogous to the $M(2)$ coordination in $C2/c$ clinopyroxenes. This eight-fold coordination is apparently achieved by two rearrangements of the structural elements, one a relative displacement of the tetrahedral chains to bring the O(5) oxygens into the coordination sphere, and the other, a shift in y positions of the $M(4)$ cations along the two-fold b axis (x and z being fixed by the $C2/m$ symmetry). The relative chain shifts influence the β angles (Whittaker, 1960), β for Ca-rich amphiboles being greater than 104.5° and for Na-rich amphiboles, varying from 103.3 to 104.0° (Appleman, *et al.*, 1966). Thus the value of β alone is a fair indicator of the $M(4)$ content, although the occupancy of the A site does affect the β value also, a point mentioned later.

In cummingtonites and grunerites the $M(4)$ site is occupied mainly by $\mathrm{Fe^{2+}}$, and in manganoan varieties, by $\mathrm{Mn^{2+}}$. When Fe and Mn occupy this site the coordination can be considered as consisting of four short bonds (1.99 to 2.21

TABLE 8. SELECTED INTERATOMIC ANGLES (DEGREES) IN $M(1)$, $M(2)$, $M(3)$ AND A SITES COMPARED FOR EIGHT CLINOAMPHIBOLES

Atoms[a]	Tremolite Present study		Cummingtonite Ghose (1961)		Grunerite Finger and Zoltai (1967)		*C*-centered manganoan cummingtonite Present study		Primitive manganoan cummingtonite Present study		Glaucophane Papike and Clark (1968)		Hornblende Present study		Potassic richterite Present study	
	Bond angle multi-plicity	Angle	Bond angle multi-plicity	Angle	Bond angle multi-plicity	Angle	Bond angle multi-plicity	Angle	Bond angle multi-plicity	Angle[a]	Bond angle multi-plicity	Angle	Bond angle multi-plicity	Angle	Bond angle multi-plicity	Angle
O(1^u)-M(1)-O(2^u)	2	95.68(7)	2	95.57	2	94.4(2)	2	95.3(1)	1	O(1^u) O(2^u) 95.8(3) O(1^d) O(2^d) 95.1(3)	2	100.0(2)	2	95.5(2)	2	96.0(2)
O(1^u)-M(1)-O(2^d)	2	85.63(7)	2	84.13	2	85.1(2)	2	85.1(1)	1	O(1^u) O(2^d) 85.9(3) O(1^d) O(2^u) 84.4(3)	2	78.7(2)	2	82.8(2)	2	86.3(1)
O(1^u)-M(1)-O(3^u)	2	94.96(9)	2	96.38	2	95.4(2)	2	95.7(2)	1	O(1^u) O(3^u) 96.8(3) O(1^d) O(3^d) 94.1(4)	2	97.2(3)	2	97.3(2)	2	95.2(2)
O(1^u)-M(1)-O(3^d)	2	83.66(9)	2	83.92	2	85.1(2)	2	83.9(2)	1	O(1^u) O(3^d) 85.7(3) O(1^d) O(3^u) 82.2(3)	2	84.3(3)	2	84.5(2)	2	82.3(2)
O(2)-M(1)-O(2)	1	87.23(8)	1	87.65	1	86.7(2)	1	86.8(1)	1	86.9(2)	1	93.2(2)	1	85.7(2)	1	89.4(2)
O(3)-M(1)-O(3)	1	80.96(8)	1	81.81	1	81.4(3)	1	82.3(1)	1	82.1(2)	1	79.8(2)	1	81.2(2)	1	79.2(1)
O(2)-M(1)-O(3)	2	95.91(7)	2	95.28	2	96.0(2)	2	95.4(1)	1	O(2^u) O(3^u) 95.9(2) O(2^d) O(3^d) 95.0(3)	2	93.6(2)	2	96.6(2)	2	95.8(1)
O(1)-M(2)-O(1)	1	79.95(7)	1	79.9	1	78.8(2)	1	80.3(1)	1	80.8(2)	1	80.0(2)	1	79.4(2)	1	78.5(1)
O(1^u)-M(2)-O(2^u)	2	92.11(7)	2	91.8	2	91.5(2)	2	92.3(1)	1	O(1^u) O(2^u) 92.8(3) O(1^d) O(2^d) 92.5(3)	2	89.6(2)	2	93.2(2)	2	90.3(1)
O(1^u)-M(2)-O(2^d)	2	83.74(7)	2	83.4	2	84.0(2)	2	84.0(1)	1	O(1^u) O(2^d) 84.0(2) O(1^d) O(2^u) 83.7(2)	2	83.0(2)	2	83.0(2)	2	82.1(1)
O(1)-M(2)-O(4)	2	92.83(6)	2	93.0	2	95.2(2)	2	92.2(1)	1	O(1^u) O(4^u) 91.6(3) O(1^d) O(4^d) 92.9(3)	2	89.9(2)	2	91.8(2)	2	92.1(1)
O(2^u)-M(2)-O(4^u)	2	90.25(8)	2	97.6	2	98.5(2)	2	95.2(1)	1	O(2^u) O(4^u) 94.1(3) O(2^d) O(4^d) 96.2(3)	2	90.4(3)	2	90.3(2)	2	89.2(2)
O(2^u)-M(2)-O(4^d)	2	93.40(7)	2	86.7	2	85.6(2)	2	88.1(1)	1	O(2^u) O(4^d) 86.6(3) O(2^d) O(4^u) 89.3(3)	2	95.8(3)	2	92.9(2)	2	97.3(2)
O(4)-M(2)-O(4)	1	95.00(8)	1	94.1	1	91.0(2)	1	95.3(1)	1	94.8(3)	1	100.9(3)	1	97.9(2)	1	98.5(2)
O(1^u)-M(3)-O(1^u)	2	97.09(6)	2	98.9	2	99.8(2)	2	97.0(1)	1	O(1^u) O(1^u) 96.7(3) O(1^d) O(1^d) 96.1(3)	2	102.9(2)	2	99.8(2)	2	96.1(1)
O(1^u)-M(3)-O(1^d)	2	82.91(7)	2	81.1	2	80.2(2)	2	83.0(1)	2	83.6(2)	2	77.1(2)	2	80.2(2)	2	83.9(1)
O(1^u)-M(3)-O(3^u)	4	95.86(6)	4	95.9	4	95.5(2)	4	95.8(1)	2	O(1^u) O(3^u) 95.2(3) O(1^d) O(3^d) 97.2(3)	4	95.8(2)	4	97.4(2)	4	96.8(1)
O(1^u)-M(3)-O(3^d)	4	84.14(6)	4	84.1	4	84.5(2)	4	84.2(1)	2	O(1^u) O(3^d) 85.1(3) O(1^d) O(3^u) 82.5(3)	4	84.2(2)	4	82.6(2)	4	83.2(1)
O(7)-O(7)-O(7)		65.91(7)		57.9		59.2(2)		60.3(1)		60.4(2)		66.8(2)		64.5(2)		69.9(1)
Δ		0.268		0.356		0.342		0.330		0.329		0.258		0.283		0.223

[a] The superscript notation u = up, d = down refers to oxygen x values greater (u) or less (d) than the x of M. The angle O(7)-O(7)-O(7) is the acute angle between two O(7) atoms in the lower chain and one O(7) in the upper chain. The angle $\Delta = 90° - ∡[\text{O(7)-O(7)-O(7)}]°/90°$, and is a measure of the displacement of the upper six-membered tetrahedral ring relative to the lower; $\Delta = 0$ would indicate that the upper ring is directly above the lower ring.

TABLE 9. ANISOTROPIC TEMPERATURE FACTOR COEFFICIENTS FOR TREMOLITE[a]

Atom	β_{11}	β_{22}	β_{33}	β_{12}	β_{13}	β_{23}
$M(1)$	0.00094(8)	0.00022(2)	0.00363(33)	0	0.00063(14)	0
$M(2)$	0.00079(8)	0.00020(2)	0.00376(33)	0	0.00076(13)	0
$M(3)$	0.00103(12)	0.00014(3)	0.00412(48)	0	0.00055(20)	0
$M(4)$	0.00168(5)	0.00036(1)	0.00602(19)	0	0.00247(8)	0
$T(1)$	0.00045(4)	0.00014(1)	0.00230(17)	−0.00006(2)	0.00044(7)	−0.00006(4)
$T(2)$	0.00039(4)	0.00017(1)	0.00195(17)	−0.00010(2)	0.00037(7)	−0.00007(4)
O(1)	0.00084(12)	0.00030(3)	0.00345(46)	0.00004(5)	0.00045(19)	−0.00003(10)
O(2)	0.00065(11)	0.00035(3)	0.00463(48)	0.00001(5)	0.00068(19)	0.00001(10)
O(3)	0.00109(17)	0.00033(5)	0.00525(72)	0	0.00096(29)	0
O(4)	0.00159(13)	0.00026(3)	0.00592(51)	−0.00028(5)	0.00125(21)	−0.00028(11)
O(5)	0.00093(12)	0.00050(3)	0.00378(48)	−0.00014(5)	0.00053(20)	0.00048(11)
O(6)	0.00082(12)	0.00051(3)	0.00364(47)	−0.00002(5)	0.00055(20)	−0.00060(11)
O(7)	0.00086(17)	0.00017(4)	0.00932(78)	0	0.00144(30)	0

[a] See text for the form of the temperature factor.

Å) and two long ones (2.51 to 2.76 Å). The O(5) oxygens have now moved completely outside the $M(4)$ coordination sphere, so the β angles are much smaller, less than 102.7°. Even the $M(4)$-O(6) distances are rather long, and obviously the four strongest bonds are to O(2) and O(4), Fe and Mn having shifted along the b axis towards the octahedral strips to achieve the short $M(4)$-O(2) distances. The significantly different coordination requirements reflected in the large differences in $M(4)$-O(2), O(4) distances in (Mg, Fe^{2+}, Mn)-amphiboles compared with (Ca, Na)-amphiboles helps explain the miscibility gap between these two groups at low temperatures. This miscibility gap is directly analogous to that observed between the clinopyroxenes, pigeonite and augite. In the primitive cummingtonite the $P2_1/m$ symmetry allows the $M(4)$ cations to be displaced from the two-fold axis and the two chains (A and B) can distort independently. Both Mg and Ca can then be accommodated in the site.

The A site. Although this site is vacant in six of the eight amphiboles being considered, the A-O distances (Table 7) have been calculated from a hypothetical atom at the A-site central point of $\frac{1}{2}$, 0, 0 to the nearby O(5), O(6) and O(7) atoms (Fig. 1) so that the changes in the geometry of the site can be followed. The vacant sites are most irregular in the (Mg, Fe^{2+}, Mn) amphiboles, as shown by the differences in distances between the long and short O(7)-O(7) diagonals (twice the A-O(7) distances, Table 7, Fig. 6). The $O(7)^d$-$O(7)^d$-$O(7)^u$ angles (Table 8, Fig. 6) also provide a measure of the site distortion; the value

$$\Delta = \frac{90° - \angle\,[O(7)\text{-}O(7)\text{-}O(7)]}{90°}$$

is a convenient index of distortion, because $\Delta = 0$ if O(7)-O(7)-O(7) = 90°, corresponding to a regular A site, and $\Delta = 1$ if O(7)-O(7)-O(7) = 0°, corresponding to a collapsed A site. Inspection of the various Δ values (Table 8) shows that the A sites are more regular in calcic and sodic amphiboles than in the (Mg, Fe^{2+}, Mn) amphiboles. The occupancy of the A site does affect the β angle, for in sodic richterite $\beta = 104°\ 10'$ (Papike, Clark and Huebner, 1968) and in potassic richterite $\beta = 104°\ 59'$.

The most regular A site is found in potassic richterite where the site is filled with K and $\Delta = 0.223$, O(7)-O(7)-O(7) = 69.9°. Even in richterite, however, the site is not as regular as the analogous site in the mica structure (Takeda and Donnay, 1966; Güven and Burnham, 1967; Güven, 1968). The higher irregularity in the amphibole structure is caused by the inherent offset created by the packing of the interlayer octahedral strips. This offset is responsible for a close approach of two O(7) atoms along the short diagonal, and is considered an important factor in producing the observed positional displacement of Na and K atoms from the A-site central point.

Another important factor particularly affecting Na because of its smaller size is the presence of Al in the tetrahedral sites. Charge-balance considerations indicate that Na may be displaced from the mirror plane along b in order to approach Al-rich tetrahedra more closely. Such behavior would be directly analogous to that observed for (Ca + Pb) in joesmithite, where displacement towards Be tetrahedra was observed (Moore, 1969). On the other hand, potassium is much larger than Na and so may be forced to displace off the twofold axis in a direction more closely aligned to the mirror plane. Gibbs and Prewitt (1966) have suggested that the direction of displacement of Na in the A site is also controlled by the O(3) anion which may be either F^- or OH^-. They found that Na was displaced along b when O(3) contained OH^- but along the mirror plane when O(3) contained F^-. Our results for the hornblende do not provide further information on this point.

The T1 and T2 tetrahedral sites. The $T(1)$ and $T(2)$ tetrahedra are quite distinct structurally (Papike and Clark, 1968). $T(1)$ is smaller and more nearly regular, corresponding to tetrahedra in mica structures with three bridging oxygen atoms. $T(2)$ is larger and more distorted, corresponding to tetrahedra in pyroxene structures with two bridging and two nonbridging oxygens. The $T(2)$-O distances to bridging oxygens O(5) and O(6) are usually longer than to nonbridging oxygens O(2) and O(4). These differences are in accord with those required by the d-p π bonding theory proposed by Cruickshank (1961). However, Clark, Appleman and Papike (1969) show that the differences in pyroxene tetrahedra are enhanced by change of the $M2$ pyroxene cation species. Only small differences between bridging and nonbridging distances occur in lithium and sodium pyroxenes but much larger differences occur in calcium pyroxenes. In the amphiboles similar relationships hold, large distortions being found in the $T(2)$ tetrahedra of tremolite and potassic richterite and smaller distortions in those of the $C2/m$ (Mg, Fe^{2+}, Mn) clinoamphiboles (Table 5). The large O(2)-$T(2)$-O(4) angle of about 116 to 119° (Table 6) is directly analogous to the O(1)-T-O(2) angle observed in the pyroxene tetrahedra. Gibbs (1969) discussed the distortions of amphibole tetrahedra in terms of d-p π-bond formation. Although tetrahedral distortions may result from both ionic bonding and covalent bonding effects, our results for both pyroxenes and amphiboles indicate that these distortions can be explained on the basis of an ionic model without resorting to d-p π bonding effects.

Comparison of the bond distances and angles found in the crystal structure of potassic richterite with those for clinoamphiboles with vacant A sites demonstrates that distortions in $T(2)$ tetrahedra may depend not only on the $M(4)$ charge requirements but also on the charge requirements of the atoms occupying the A site. The long distances from $T(2)$ to O(5) and O(6) and from $T(1)$ to O(7) (Table 5) are in the right direction to satisfy the charge of potassium in the A site. Because there is little or no tetrahedral aluminum in richterites, the method of charge compensation of their A sites has long been a subject of concern. It is apparent that tetrahedral distortions involving the long bonds of Si to O(5), O(6) and O(7) oxygens provide at least part of the answer.

We now consider those amphiboles containing appreciable amounts of tetrahedral Al and the apparent 25 percent limit that is observed. If Al were restricted to $T(1)$ (Fig. 1) and more than 25 percent tetrahedral Al were present, Al-O-Al linkages would have to form. Numerous structural investigations on silicates demonstrate that while such linkages can form in certain instances they are usually avoided. In amphiboles such linkages can be avoided either by having less than 25 percent tetrahedral Al in the ordered structure or by the introduction of some tetrahedral Al into $T(2)$. The 25 percent limit may also be related to the kind of cation occupying the A site. If the site is entirely filled by univalent cations, Na$^+$ or K$^+$, the charge balance requires a maximum of 25 percent tetrahedral Al (although there may be much less, as indicated by the potassic richterite analysis, Table 1). If small amounts of Ca^{2+} enter the A site, slightly more than 25 percent tetrahedral Al may be accommodated. If half the $T(1)$ sites were ordered with respect to Al and Al-O-Al linkages were avoided, the mirror plane would be lost. The $C2/m$ symmetry would then be lowered, possibly to $P2/a$ as in joesmithite (Moore, 1969) or to $C2$, and the relationships of the tetrahedral chains throughout the cell would be changed accordingly.

TABLE 10. MAGNITUDES AND ORIENTATIONS OF THE PRINCIPAL AXES OF THE THERMAL ELLIPSOIDS IN TREMOLITE

Atom	Ellipsoid axis	rms amplitude, Å	Angles, degrees with respect to		
			a	b	c
$M(1)$	r_1	0.060(3)	90	0	90
	r_2	0.063(4)	22(19)	90	127(19)
	r_3	0.070(3)	68(19)	90	37(19)
$M(2)$	r_1	0.055(5)	162(9)	90	58(9)
	r_2	0.057(3)	90	0	90
	r_3	0.072(3)	72(9)	90	32(9)
$M(3)$	r_1	0.048(5)	90	0	90
	r_2	0.068(5)	178(40)	90	77(40)
	r_3	0.074(4)	92(40)	90	13(40)
$M(4)$	r_1	0.048(4)	143(1)	90	39(1)
	r_2	0.077(1)	90	0	90
	r_3	0.105(1)	53(1)	90	51(1)
$T(1)$	r_1	0.036(4)	143(6)	123(6)	64(6)
	r_2	0.052(2)	126(8)	37(12)	88(20)
	r_3	0.056(2)	82(15)	77(19)	26(6)
$T(2)$	r_1	0.031(4)	147(4)	119(4)	64(6)
	r_2	0.051(2)	108(8)	86(12)	147(9)
	r_3	0.058(2)	117(5)	29(5)	72(12)
O(1)	r_1	0.061(5)	18(25)	108(23)	104(127)
	r_2	0.067(4)	94(34)	104(43)	157(38)
	r_3	0.072(4)	107(18)	157(33)	71(43)
O(2)	r_1	0.052(6)	177(8)	89(9)	73(8)
	r_2	0.076(3)	89(10)	8(73)	98(70)
	r_3	0.078(4)	88(9)	82(74)	19(34)
O(3)	r_1	0.066(8)	166(15)	90	62(15)
	r_2	0.074(6)	90	0	90
	r_3	0.084(5)	76(15)	90	28(15)
O(4)	r_1	0.054(5)	62(7)	29(5)	90(8)
	r_2	0.079(6)	49(9)	105(9)	148(8)
	r_3	0.098(3)	54(7)	115(4)	58(8)
O(5)	r_1	0.054(8)	135(14)	118(5)	47(12)
	r_2	0.068(4)	130(14)	82(8)	124(12)
	r_3	0.099(3)	106(4)	29(4)	63(4)
O(6)	r_1	0.060(6)	173(23)	92(6)	69(24)
	r_2	0.069(4)	97(24)	90(8)	159(24)
	r_3	0.092(3)	88(5)	178(5)	91(16)
O(7)	r_1	0.053(6)	90	0	90
	r_2	0.056(9)	3(5)	90	107(5)
	r_3	0.111(5)	87(5)	90	17(5)

The geometry of the tetrahedral chains. The O(5)-O(6)-O(5) angle in the tetrahedral chains (Table 6, Fig. 1) varies between 167.6° and 172.9° for tremolite, cummingtonite, grunerite, *C*-centered manganoan cummingtonite, glaucophane and potassic richterite, but lies outside this range for primitive manganoan cummingtonite and hornblende. The straightest chain (chain A) is found in primitive manganoan cummingtonite with an O(5)-O(6)-O(5) angle of 178.4°, and the greatest kinking is observed in hornblende with an O(5)-O(6)-O(5) angle of 163.1°. The significant kinking in the aluminous hornblende tetrahedral chains is required to fit the fairly large Al-rich tetrahedra to the octahedral strip.

Charge balance in clinoamphiboles. In order to examine the charge balance associated with the oxygen atoms using Pauling's second rule (Pauling, 1929), it is convenient to divide the clinoamphiboles into two groups, one with the *A* site vacant, and the other, with the *A* site occupied. In both cases oxygens O(1), O(2) and hydroxyl O(3) are always found to receive about 2.0 valence units (v.u.) according to the ideal model (a slight excess would be associated with O(1) for glaucophane). However, oxygen O(4) is always deficient, receiving only 1.6 v.u. Because O(5), O(6) and O(7) coordinate the *A* site, their compensation depends on the kind of atom occupying that site and the coordination assumed. For clinoamphiboles with vacant *A* sites, O(7) receives 2.00 v.u. but O(5) and O(6) have a slight excess, receiving from 2.1 to 2.3 v.u. When the *A* site is occupied by a univalent cation, these three oxygens all receive from 2.2 to 2.4 v.u. on the basis of this model.

If the empirical relationships for bond strength *vs* bond distance developed for clinopyroxenes by Clark, Appleman and Papike (1969) are applied to tremolite, glaucophane, and K-richterite, each oxygen is found to receive very nearly 2.0 v.u. The bond distances are thus in the right direction to obtain the necessary charge balance. Furthermore, for K-richterite the empirical relationships indicate better charge balance for K when the split-atom model with 8-coordination is assumed, despite a slight charge deficiency obtained for K in either case. The K-O bond strength *vs* bond distance curve was assumed to be similar to that used for Na-O in the pyroxenes, so the errors involved may be partly responsible for the calculated deficiency. However, the improvement found for the split-atom model lends some support to the hypothesis of positional rather than thermal disorder for the A-site occupant.

SUMMARY AND CONCLUSIONS

The most important conclusions are the following:

1. The occupancy of the *M*(4) cation site is of key importance in amphibole phase relations. Significant differences exist between the *M*(4)-O coordination polyhedra in (Mg, Fe^{2+}, Mn) clinoamphiboles and (Ca, Na) amphiboles, and these differences are believed to be largely responsible for the limited miscibility between these amphibole groups at low temperatures. The presence of Mg together with Ca or Na in this site is considered responsible for the occurrence of the primitive clinoamphibole structure.

2. The primitive clinoamphibole structure has space-group symmetry $P2_1/m$ and contain two symmetrically distinct tetrahedral chains, A and B. Chain A is relatively straight with an O5-O6-O5 angle of 178° and chain B is relatively kinked with an O(5)-O(6)-O(5) angle of 166°. The structure has the same number of *M* sites as $C2/m$ amphiboles, but each site has two more degrees of positional parameter freedom.

3. The details of the $P2_1/m$ structure bear certain relationships to those of anthophyllite, and anthophyllite may be considered as approximately built from blocks of the $P2_1/m$ structure with an ABAB stacking sequence where B is related to A by 180° rotation around a^*. The $P2_1/m$ structure is the closest known one to anthophyllite that can be produced from a $C2/m$ structure without breaking bonds; it is the amphibole analog of the $P2_1/c$ clinopyroxene, pigeonite.

4. Potassic richterite represents a crystal-chemical "end-member" amphibole with its *A* site filled with potassium. This potassium can be exchanged for sodium in KCl and NaCl melts, and NaOH and KOH solutions. Sodium-potassium exchange in amphiboles follows one-dimensional exchange paths compared with two-dimensional paths in micas, and three-dimensional ones in feldspars.

5. The K atoms in richterite and the (Na, K) atoms in hornblende are best represented by a split-atom model, indicating either thermal or positional disorder around the *A* site central point (1/2, 0, 0).

6. On the basis of the split-atom model, the potassium coordination is tighter in clinoamphiboles, with eight oxygen neighbors at less than 3.00 Å, than in micas with only six oxygen neighbors in that range. This result tends to support the idea of the occurrence of potassic amphiboles in the high-pressure environment of the upper mantle.

7. The *T*(1) tetrahedron in clinoamphiboles is smaller and more regular than *T*(2) and is analogous to tetrahedra in micas with three bridging oxygens.

8. The *T*(2) tetrahedron in clinoamphiboles is larger and more distorted than *T*(1) and is analogous to tetrahedra in pyroxenes with two bridging and two nonbridging oxygen atoms. The distortions in the *T*(2) tetrahedra can be explained satisfactorily by the ionic effects resulting from the chemical species occupying the *M*(4) and *A* sites.

9. The *T*(1) tetrahedron in hornblende is enriched in aluminum relative to *T*(2), and the observed *T*-O distances provide an indication of the lengthening to be expected in the presence of aluminum.

10. A reasonable isotropic temperature factor for Mg in octahedral coordination in clinoamphiboles is 0.32 $Å^2$.

11. In tremolite, an ordered clinoamphibole, there is ap-

preciable thermal anisotropy observed only for the $M(4)$ occupant, Ca.

12. Refinement of the tremolite structure has given the first X-ray diffraction evidence for the location of the hydrogen atom in an amphibole. It lies in the mirror plane with the O(3)-H distance of 0.87(7) Å and makes an angle of approximately 94(4)° with the octahedral strip.

13. Results of the refinement of *C*-centered manganoan cummingtonite, when combined with previous X-ray and spectral results for cummingtonite and grunerite, demonstrate the $M(4)$ site preference as $Mn^{2+} > Fe^{2+} > Mg$.

ACKNOWLEDGEMENTS

We appreciate the help of many who have contributed to this study. Dr. C. Klein, Harvard University, provided the manganoan cummingtonite sample and Dr. B. Mason, U. S. National Museum, supplied the hornblende and potassic richterite samples. Dr. A. T. Anderson, U.S. Geological Survey (now at the University of Chicago) did the electron-probe microanalyses on primitive manganoan cummingtonite, and Dr. J. J. Fahey, U.S. Geological Survey, the wet chemical analysis of tremolite. Dr. R. W. T. Wilkins, University of Queensland, Australia, provided information about the infrared spectra of primitive manganoan cummingtonite in advance of publication. Dr. L. W. Finger, Geophysical Laboratory, made computer programs available for the site occupancy refinement of *C*-centered manganoan cummingtonite and thermal ellipsoid calculations in tremolite. He, together with Dr. Daniel E. Appleman, U. S. Geological Survey, were both helpful on computational aspects of this research and in discussions about amphibole crystal Chemistry. Mrs. Judith A. Konnert, U. S. Geological Survey, merits special thanks for technical assistance throughout this study.

REFERENCES

APPLEMAN, D. E., F. R. BOYD, G. M. BROWN, W. G. ERNST, G. V. GIBBS, AND J. V. SMITH (1966) *Short Course on Chain Silicates*. Amer. Geol. Inst., Washington, D.C.

BANCROFT, G. M., R. G. BURNS, AND A. G. MADDOCK (1967) Determination of cation distribution in the cummingtonite-grunerite series. *Amer. Mineral.* **52,** 1009–1026.

BOWN, M. G. (1965) A new amphibole polymorph in intergrowth with tremolite: clino-anthophyllite? [abstr.]. *Amer. Mineral.* **51,** 259–260 (1966).

BURNHAM, CHARLES W. (1967) Ferrosilite. *Carnegie Inst. Year Book* **65,** 285–290.

BURNS, R. G., AND R. G. J. STRENS (1966) Infrared study of the hydroxyl bands in clinoamphiboles. *Science* **153,** 890–892.

CARMICHAEL, I. S. E. (1967) The mineralogy and petrology of the volcanic rocks from the Leucite Hills, Wyoming. *Contrib. Mineral. Petrology* **15,** 24–66.

CLARK, JOAN R., AND J. J. PAPIKE (1968) Crystal-chemical characterization of omphacites. *Amer. Mineral.* **53,** 840–868.

———, D. E. APPLEMAN, AND J. J. PAPIKE (1969) Crystal-chemical characterization of clinopyroxenes based on eight new structure refinements. *Mineral. Soc. Amer. Spec. Pap.* **2,** 31–50.

COLVILLE, A. A. AND G. V. GIBBS (1964) Refinement of the crystal structure of riebeckite [abstr.]. *Geol. Soc. Amer. Spec. Pap.* **82,** 31 (1965).

———, AND P. H. RIBBE (1968) The crystal structure of an adularia and a refinement of the structure of orthoclase. *Amer. Mineral.* **53,** 25–37.

CRUICKSHANK, D. W. J. (1961) The role of $3d$-orbitals in π-bonds between (a) silicon, phosphorous, sulphur, or chlorine and (b) oxygen or nitrogen. *J. Chem. Soc.* **1961,** 5486–5504.

DEVORE, G. W. (1957) The association of strongly polarizing cations with weakly polarizing cations as a major influence in element distribution, mineral composition, and crystal growth. *J. Geol.* **65,** 178–195.

FINGER, L. W., AND T. ZOLTAI (1967) Cation distribution in grunerite [abstr.]. *Trans. Amer. Geophys. Union* **48,** 233–234.

FISCHER, K. F. (1966) A further refinement of the crystal structure of cummingtonite, $(Mg, Fe)_7 (Si_4O_{11})_2 (OH)_2$. *Amer. Mineral.* **51,** 814–818.

FREED, R. L., AND DONALD R. PEACOR (1967) Refinement of the crystal structure of johannsenite. *Amer. Mineral.* **52,** 709–720.

GHOSE, S. (1961) The crystal structure of cummingtonite. *Acta Crystallogr.* **14,** 622–627.

——— (1965) A scheme of cation distribution in the amphiboles. *Mineral. Mag.* **35,** 46–54.

———, AND E. HELLNER (1959) The crystal structure of grunerite and observations on the Mg-Fe distribution. *J. Geol.* **67,** 691–701.

GIBBS, G. V. (1969) The crystal structure protoamphibole. *Mineral. Soc. Amer. Spec. Pap.* **2,** 101–110.

———, AND C. T. PREWITT (1966) Amphibole cation site disorder [abstr.]. *In Int. Mineral. Ass. Pap. Proc. 5th Gen. Meet. Mineralogical Society, London* (1968), p. 334.

GÜVEN, NECIP (1968) The crystal structures of $2M_1$ phengite and $2M_1$ muscovite. *Carnegie Inst. Year Book* **66,** 487–492.

———, AND CHARLES W. BURNHAM (1967) The crystal structure of $3T$ muscovite. *Z. Kristallogr.* **125,** 163–183.

HERITSCH, H., AND E. KAHLER (1960) Strukturuntersuchung an zwei Kluftkarinthinen, Ein Beitrag zur Karinthinfrage. *Tschermak's Mineral. Petrog. Mitt.* **7,** 218–234.

———, AND L. RIECHERT (1960) Strukturuntersuchung an einer basaltischen Hornblende von Cernosin, CSR. *Tschermak's Mineral. Petrog. Mitt.* **7,** 235–245.

———, G. BERTOLDI, AND E. M. WALITZI (1960) Strukturuntersuchung in einer basaltischen Hornblende vom Kuruzzenkogel, südlich Fehring, Steirmark. *Tschermak's Mineral. Petrog. Mitt.* **7,** 210–217.

———, P. PAULITSCH, AND E. M. WALITZI (1957) Die Struktur von Karinthin und einer barroisitschen Hornblende. *Tschermak's Mineral. Petrog. Mitt.* **6,** 215–225.

KAWAHARA, A. (1963) X-ray studies on some alkaline amphiboles. *Mineral. J. [Tokyo]* **4,** 30–40.

KLEIN, C. (1964) Cummingtonite-grunerite series: A chemical, optical and X-ray study. *Amer. Mineral.* **49,** 963–982.

MACGILLAVRY, C. H. AND G. D. RIECK (eds.) (1962) *International Tables for X-ray Crystallography, Vol. 3.* Kynoch Press, Birmingham.

MASON, B. (1966) Pyrope, augite, and hornblende from Kakanui, New Zealand. *N. Z. J. Geol. Geophys.* **9,** 474–480.

——— (1968) Eclogitic xenoliths from volcanic breccia at Kakanui, New Zealand. *Contrib. Mineral. Petrology* **19,** 316–327.

MOORE, PAUL B. (1969) Joesmithite: a novel amphibole crystal chemistry. *Mineral. Soc. Amer. Spec. Pap.* **2,** 111–115.

OXBURGH, E. R. (1964) Petrological evidence for the presence of amphibole in the upper mantle and its petrogenetic and geophysical implications. *Geol. Mag.* **101,** 1–19.

PAPIKE, J. J., AND JOAN R. CLARK (1967) Crystal-chemical role of potassium and aluminum in a hornblende of proposed mantle origin (abstr.). *Geol. Soc. Amer. Prog. 1967 Ann. Meet., New Orleans* [*Geol. Soc. Amer. Spec. Pap.* **115,** 171 (1968)].

———, AND ——— (1968) The crystal structure and cation distribution of glaucophane. *Amer. Mineral.* **53,** 1156–1173.

———, ———, AND J. S. HUEBNER (1968) Potassic richterite, $KNaCaMg_5Si_8O_{22}(OH, F)_2$: crystal chemistry and sodium-potassium exchange (abstr.). *Geol. Soc. Amer., Prog. 1968 Ann. Meet., Mexico City. Geol. Soc. Amer. Spec. Pap.* **121,** 230 (1969)].

———, M. ROSS, AND J. R. CLARK (1968) Crystal-chemical and petrologic significance of the $P2_1/m$ amphibole analog of pigeonite (abstr.). *Trans. Amer. Geophys. Union* **49,** 340–341.

PAULING, LINUS (1929) The principles determining the structure of complex ionic crystals. *J. Amer. Chem. Soc.* **51,** 956–975.

PREWITT, C. T. (1963) Crystal structures of two synthetic amphiboles (abstr.). *Geol. Soc. Amer. Prog. 1963 Ann. Meet.* [*Geol. Soc. Amer. Spec. Pap.* **76,** 132–133 (1964)].

PRIDER, R. T. (1939) Some minerals from the leucite-rich rocks of the West Kimberly area, Western Australia. *Mineral. Mag.* **25,** 373–387.

ROSS, M., J. J. PAPIKE, AND K. W. SHAW (1969) Exsolution textures in amphiboles as indicators of subsolidus thermal histories. *Mineral. Soc. Amer. Pap.* **2,** 275–299.

———, ———, AND P. W. WEIBLEN (1968) Exsolution in clinoamphiboles. *Science* **159,** 1099–1102.

———, W. L. SMITH, AND W. H. ASHTON (1968) Triclinic talc and associated amphiboles from Gouverneur Mining District, New York. *Amer. Mineral.* **53,** 751–769.

SEGELER, C. G. (1961) First U. S. occurrence of manganoan cummingtonite, tirodite. *Amer. Mineral.* **46,** 637–641.

SMITH, J. V. (1954) A review of the Al-O and Si-O distances. *Acta Crystallogr.* **7,** 479–481.

———, AND S. W. BAILEY (1963) Second review of *Al*-O and Si-O tetrahedral distances. *Acta Crystallogr.* **16,** 801–811.

TAKEDA, H., AND J. D. H. DONNAY (1965) Trioctahedral one-layer micas. III. Crystal structure of a synthetic lithium fluormica. *Acta Crystallogr.* **20,** 638–646.

WARREN, B. E. (1929) The structure of tremolite $H_2Ca_2Mg_5(SiO_3)_8$. *Z.* **72,** 42–57.

WHITTAKER, E. J. W. (1949) The structure of Bolivian crocidolite. *Acta Crystallogr.* **2,** 312–317.

——— (1960) The crystal chemistry of the amphiboles. *Acta Crystallogr.* **13,** 291–298.

ZUSSMAN, J. (1955) The crystal structure of actinolite. *Acta Crystallogr.* **8,** 301–308.

——— (1959) A re-examination of the structure of tremolite. *Acta Crystallogr.* **12,** 309–312.